Lipid-Gramicidin Interactions Using Two-Dimensional Fourier-Transform Electron Spin Resonance

Baldev R. Patyal, Richard H. Crepeau, and Jack H. Freed
Baker Laboratory of Chemistry, Cornell University, Ithaca, New York 14853 USA

ABSTRACT The application of two-dimensional Fourier-transform electron-spin-resonance (2D-FT-ESR) to the study of lipid/gramicidin A (GA) interactions is reported. It is shown that 2D-FT-ESR spectra provide substantially enhanced spectral resolution to changes in the dynamics and ordering of the bulk lipids (as compared with cw-ESR spectra), that result from addition of GA to membrane vesicles of dipalmitoylphosphatidylcholine (DPPC) in excess water containing 16-PC as the lipid spin label. The agreement between the theory of Lee, Budil, and Freed and experimental results is very good in the liquid crystalline phase. Both the rotational and translational diffusion rates of the bulk lipid are substantially decreased by addition of GA, whereas the ordering is only slightly increased, for a 1:5 ratio of GA to lipid. The slowing effect on the diffusive rates of adding GA in the gel phase is less pronounced. It is suggested that the spectral fits in this phase would be improved with a more detailed dynamic model. No significant evidence is found in the 2D-FT-ESR spectra for a second immobilized component upon addition of GA, which is in contrast to cw-ESR. It is shown from simulations of the observed 2D-FT-ESR spectra that the additional component seen in cw-ESR spectra, and usually attributed to "immobilized" lipid, is inconsistent with its being characterized by increased ordering, according to a model proposed by Ge and Freed, but it would be consistent with the more conventional model of a significantly reduced diffusional rate. This is because the 2D-FT-ESR spectra exhibit a selectivity, favoring components with longer homogeneous relaxation times, T_2. The homogeneous linewidths of the 2D-FT-ESR autopeaks appear to broaden as a function of mixing time. This *apparent* broadening is very likely due to the process of cooperative order director fluctuations (ODF) of the lipids in the vesicle. This real-time observation of ODF is distinct from, but appears in reasonable agreement with, NMR results. It is found that addition of GA to give the 1:5 ratio has only a small effect on the ODF, but there is a significant temperature dependence.

INTRODUCTION

Two-dimensional Fourier transform (2D-FT) electron-spin-resonance (ESR) was recently introduced as a technique that provides considerable enhancement in resolution to ordering and dynamics as compared to conventional ESR spectroscopy in studies of nitroxide-labeled lipids and cholesterol in membrane vesicles (Crepeau et al., 1994; Lee et al., 1994a). While ESR has played an important role in understanding the dynamics and structure of membranes in many past studies (Devaux and Seignenret, 1985; Marsh, 1985, 1989; Kar et al., 1985; Freed, 1987; Ge et al., 1994) there is generally poor spectral resolution in typical ESR studies on membrane vesicles (Meirovitch et al., 1984; Ge and Freed, 1993). This poor resolution is largely due to the fact that these samples are characterized by the lipids being *m*icroscopically *o*rdered, within the vesicle, but the sample is *m*acroscopically *d*isordered, (i.e., a vesicle dispersion), which we refer to as MOMD. As a result, there is a superposition of spectra from membrane fragments that are randomly oriented. In addition, there is inhomogeneous broadening due to proton superhyperfine (shf) interactions, which further reduces the resolution to the homogeneous line broadening that supplies the spin-relaxation and motional dynamic information. In principle, the MOMD effect on the linewidths and lineshapes, and how it varies from one hf line to another, can be utilized to obtain information about the ordering, but it is difficult to deconvolute from the effects of proton shf broadening as well as from the motional broadening, even with detailed spectral simulations (Ge and Freed, 1993). However, by using 2D-FT-ESR methods the extra spectral dimension, as well as the ability of the spin echo to cancel inhomogeneous broadening, leads to the significantly increased resolution (Crepeau et al., 1994; Lee et al., 1994a, b).

We briefly outline how this increased spectral resolution is achieved. A characteristic shared by all 2D-FT-ESR experiments based on collection of free-induction decays (FIDs) is that one detects a dual quadrature signal, i.e., a signal that is complex, with a real absorptive part and an imaginary dispersive part, with respect to each frequency in the 2D representation (Gorcester et al., 1990). This "hypercomplex" signal can be combined to give two ordinary complex signals that we call S_{c+} and S_{c-}. The first (the S_{c+} signal) is FID-like, because it is not refocused by the last or "read-out" pulse, whereas the second (the S_{c-} signal) is echo-like because it is refocused by the last pulse (Gamliel and Freed, 1990). In the absence of inhomogeneous broadening, the two are of course identical. In the presence of inhomogeneous broadening the S_{c+} and S_{c-} signals are

Received for publication 10 March 1997 and in final form 23 June 1997.

Address reprint requests to Dr. Jack H. Freed, Department of Chemistry, Cornell University, B52 Baker Lab, Ithaca, NY 14853-1301. Tel.: 607-255-3647; Fax: 607-255-0595; E-mail: jhf@msc.cornell.edu.

Dr. Patyal's present address is Research Imaging Center, University of Texas Health Sciences Center, 7703 Floyd Curl Drive, San Antonio, TX 78284.

0006-3495/97/10/2201/20 $2.00

quite different, with the S_{c-} spectra being substantially sharper due to an echo-like cancellation of the inhomogeneities, which does not occur for the S_{c+} spectra. In the two-pulse, or COSY experiment, a comparison of the S_{c+} and S_{c-} spectra will provide useful information to distinguish homogeneous from inhomogeneous broadening, and the variation of the inhomogeneous broadening with the hf line provides direct information on the MOMD contribution. If only the S_{c-} spectrum is available (because of the more rapid decay of the S_{c+} signal during the spectrometer dead time, since its inhomogeneous broadening is not refocused), it is still possible to obtain this same information from just the S_{c-} signal. This is because the refocusing of inhomogeneities is achieved along one spectral dimension, whereas it is not refocused along the orthogonal spectral dimension. (This is strictly true after the S_{c-} spectrum is transformed into a SECSY spectrum. cf. below.)

The three-pulse or 2D-ELDOR experiment provides even more detailed information (Gorcester et al., 1990). In this experiment, crosspeaks appear that are a measure of magnetization transfer by spin relaxation processes during the mixing time, T_m. The principal spin relaxation mechanisms are the intramolecular electron-nuclear dipolar (END) interactions, which lead to nuclear spin flip transitions (with rate W_n) that report on the rate of rotational reorientation, and the Heisenberg exchange (HE) rate, (ω_{HE}), which reports on the bimolecular collision rate of the spin-labeled molecules. The pattern of crosspeaks enables one to distinguish the contributions from each relaxation mechanism. These experiments are done as a series of different mixing times, T_m, to observe how these crosspeaks "grow-in" relative to autopeaks as a result of these cross-relaxation mechanisms. In fact, such a series of 2D spectra versus T_m provides, in effect, a third spectral dimension.

Inhomogeneous broadening plays an important role in the case of MOMD spectra from membrane vesicles in 2D-ELDOR. It is now possible to utilize the different shapes of the autopeaks and crosspeaks to precisely distinguish the contribution to inhomogeneous broadening from proton shf interactions, which is the same for each hf line, and the MOMD effect, which varies for each hf line. For autopeaks, there is an echo-like cancellation for the S_{c-} signal, but the crosspeaks that develop have a new feature. During the evolution period, t_1, a given spin label belonging to hf component "a" will evolve with the inhomogeneity associated with this hf component. After it exchanges to hf component "b" during the mixing time, T_m, it will evolve with the refocused inhomogeneity during the detection period, t_2. If the inhomogeneities associated with hf components "a" and "b" are different, as in the case for the MOMD contribution, but not for contributions from proton shfs, then their differences will show up in the crosspeak broadenings. The crosspeak shapes, compared with the autopeak shapes, therefore provide a sensitive measure of the MOMD inhomogeneity effects and hence the extent of ordering. In the case of S_{c+} 2D-ELDOR spectra, these inhomogeneities are additive for the crosspeaks as well as autopeaks, thereby supplying supplementary information.

Given the subtle interplay of various relaxation processes on the crosspeak intensities and the homogeneous linewidths, and of the various sources of inhomogeneous broadening on the auto and crosspeaks, we find that the most effective way of extracting relevant relaxation and ordering data is to perform nonlinear least squares (NLLS) fitting of the 2D spectral simulations to the experimental spectra. The detailed theory for simulating 2D-FT-ESR spectra is described elsewhere (Lee et al., 1994b). The NLLS fitting of the 2D spectra is analogous to our methods for fitting cw-ESR spectra, but is more sophisticated (Budil et al., 1996). We simultaneously fit the full 3D data set (i.e., the set of 2D spectra obtained for different mixing times, T_m). Of the extensive instrumental innovations (Gorcester et al., 1989, 1990; Patyal et al., 1990; Lee et al., 1993; Crepeau et al., 1994; Sastry et al., 1996), the short 40–50-ns spectrometer dead times proved to be very important.

In this paper we apply the enhanced resolution to ordering and dynamics of 2D-FT-ESR to study the effect of the peptide gramicidin A (GA) on a lipid membrane. In the past, lipid-protein interactions have been extensively investigated in both reconstituted and biological membranes by cw-ESR (Marsh, 1989; Devaux and Seignenret, 1985). More recently, Ge and Freed (1993) have performed detailed lineshape simulations to interpret the cw-ESR spectra from multilamellar vesicles of DPPC with varying amounts of GA containing spin-labeled lipids. This serious effort, while quite informative, was hampered by the substantial limitations to spectral resolution of the cw-ESR spectra referred to above. In the present paper we first wish to demonstrate the enhanced spectral resolution to changes in membrane ordering and dynamics induced by addition of GA that is obtained by 2D-FT-ESR spectroscopy. We then use our detailed analyses of these spectra to improve our understanding of the effects of GA on the membrane, and we also attempt to critically assess the future potential of 2D-FT-ESR in studies on the dynamic structure of membranes.

MATERIALS AND METHODS

Materials

Gramicidin A′, which is a mixture of gramicidin A, B, and C, was purchased from Sigma Chemical Company (St. Louis, MO). The phospholipid 1,2-dipalmitoyl-*sn*-glycero-phosphatidylcholine (DPPC) and the spin label 1-palmitoyl-2-(16-doxyl stearoyl) phosphatidylcholine (16-PC) were purchased from Avanti Polar Lipids, Inc. (Birmingham, AL). All materials were used without further purification.

Sample preparation

16-PC in DPPC

A measured amount of 1.9 mM 16-PC in chloroform was added to 50 mg DPPC to yield 1 mol % of spin label 16-PC in DPPC. The solution was evaporated to about half of the original volume and then ~0.05 ml of the concentrated solution was transferred to a thin-walled, 2-mm ID Pyrex sample tube. The chloroform was evaporated by desiccating at 35°C on the vacuum line for ~12 h. A small excess of water (~30% by volume) was added to the sample tube. The sample was heated to ~60°C for ~20 min to ensure complete hydration of lipid bilayers. The sample was degassed by

repeated freeze-pump-thaw cycles to 0.3 mTorr. In the final cycle, prepurified N_2 gas was leaked into the sample at ½ atmosphere and the sample tube was sealed. The last step was necessary to ensure proper hydration of the sample over a temperature range from 25°C to 80°C.

16-PC in DPPC/GA

GA (25.6 mg) was dissolved in 0.25 ml methanol. Also, 50 mg DPPC was dissolved in 0.282 ml of 2.9 mM solution of 16-PC in chloroform. The two solutions were mixed. The rest of the procedure is identical to that outlined above. This gave a 1 mol % 16-PC in DPPC/GA mixture with a DPPC to GA molar ratio of 5 to 1 plus the added water.

2D-FT-ESR experiments

All experiments reported here were performed on our pulsed ESR spectrometer, the details of which are described elsewhere (Gorcester et al., 1989, 1990; Lee et al., 1993; Crepeau et al., 1994). For the ELDOR experiments (cf. Fig. 1 *b*), three $\pi/2$ pulses were used. With 1 kW of microwave power from the TWT amplifier and a 3.25-mm ID bridged loop gap resonator, the pulse width for a $\pi/2$ pulse corresponds to ~5 ns. The loaded Q of the resonator is ~40. Under optimum conditions we obtained a uniform coverage over ±70 MHz, and a spectrometer dead time of 50 ns. Since the spectral extent for all our experiments reported in this paper never exceeded 100 MHz, (or ±50 MHz), no correction for the coverage (Crepeau et al., 1994) was needed.

The sample temperature was regulated using a gas flow type cryostat with a commercial temperature controller (Bruker, model ER4111VT) to an accuracy of ~±1°C. The magnetic field was stabilized using a standard field-frequency lock arrangement (Varian Fieldial Mark II), leading to a field stability better than ±10 mG (or about 3 parts in 10^6). The microwave frequency was stabilized to an accuracy of ~±1 kH (or about 1 part in 10^7), using a Microwave Systems Inc. Model MOS lock box.

We collected 2D-ELDOR signals over the temperature range of 25°–80°C. The short dead time, t_d = 50 ns, made it possible for us to collect signals from DPPC and DPPC/GA dispersion samples even at room temperature, where $T_2^* \sim$ 15–20 ns. The separation between the first two pulses, i.e., t_1, was stepped with 128 steps of 3 ns each, from an initial value of 50 ns. Each signal was collected as a function of t_2 for a total of 256 complex points with an effective step size of 1 ns. This step size was achieved by automatically interleaving five separate collections, each sampled with 5-ns steps using our two-channel DSP signal averager. A 32-step dual quadrature phase cycling sequence modified from the 16-step sequence of Gamliel and Freed (1990) was used to eliminate the unwanted signals such as the image peaks, transverse signals, and axial peaks. The additional 16 steps provided further elimination of instrumental artifacts that were not fully removed by the original 16-step phase cycle. A full data collection at one t_1 point consisted of 500 averages for each of the 32 phase cycle steps. A complete 2D-ELDOR experiment took ~20 min at a 10 kHz repetition rate. The full dual quadrature signal was collected and later both S_{c+} and S_{c-} components (Gamliel and Freed, 1990) were analyzed. The experiments were repeated for a series of 6–8 mixing times, T_m, ranging from 90 ns to 4 μs. For COSY experiments, the signals were collected after the second pulse and the stepping out in t_1 and t_2 was performed in exactly the same way as in the 2D-ELDOR experiment. An 8-step phase cycle sequence (Gamliel and Freed, 1990) was used to eliminate unwanted signals.

Data processing

We observed that the short dead times in t_1 and t_2 caused some instrumental artifacts in the data. The first two pulses showed some interaction as a function of their separation for the initial 150–200-ns period resulting in a slight variation in phase and width of the second pulse. The effect of this on the data was substantially suppressed by determining an instrument response function as described by Crepeau et al. (1994). All data in the liquid crystalline phase of DPPC and DPPC/GA were corrected in this manner. Data in the gel phase (below 45°C) were not corrected because in the gel phase the spectral peaks are already broader due to slower motions and increased ordering, so that the artifacts are more or less merged with the broad real peaks. Any attempt to remove the artifacts adversely affected the real data as well. In these cases, no other filtering or smoothing was needed on any of the data presented in this paper.

In preparation for the nonlinear least squares (NLLS) fitting of the spectra to the theoretical simulations, they were Fourier-transformed along both t_1 and t_2. The magnitude spectrum was used to avoid the need for corrections for phase variations across the 2D spectrum that result from the finite dead times and use of microwave magnetic fields of finite strength (Gorcester and Freed, 1988; Patyal et al., 1990; Lee et al., 1993). This processing was done for both the S_{c-} and S_{c+} spectra. The homogeneous T_2 values were obtained from the COSY spectra and "apparent" T_2 values

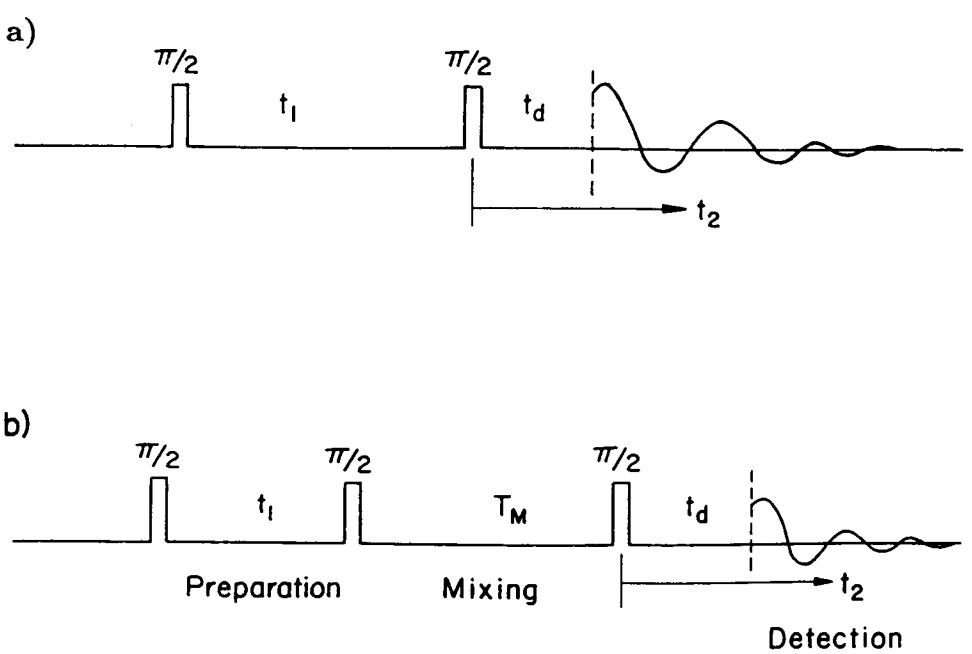

FIGURE 1 The pulse sequences used for 2D-ESR experiments: (*a*) COSY, and (*b*) ELDOR.

from the ELDOR data (Crepeau et al., 1994; Lee et al., 1994a), by transforming into the SECSY format, (i.e., a simple shear transformation: $t_2 \rightarrow t_2 + t_1$; cf. Lee et al., 1994b). The transformed data were Fourier-transformed along t_2 and then processed using linear prediction by singular value decomposition (LPSVD) along t_1. We did not see much T_2 variation across the spectrum in the COSY data, as expected from magnitude displays (cf. Lee et al., 1994b), but we saw a clear trend wherein the line broadening of the autopeaks in the ELDOR experiments initially increases with increasing mixing time, T_m, and then asymptotically levels off at longer mixing times. We found that this increase in apparent T_2^{-1} could be fit by the expression:

$$(T_2^{-1})_{app} = (T_2^{-1})_0 + \Delta_{LW}(1 - \exp(-T_m/\tau_c) \qquad (1)$$

$(T_2^{-1})_{app}$ is the measured or apparent linewidth, $(T_2^{-1})_0$ is the linewidth at mixing time $T_m = 0$, and (τ_c^{-1}) is the rate of "growing-in" of the additional broadening, Δ_{LW}.

Nonlinear least squares simulations

The Fourier-transformed magnitude spectra were analyzed to obtain the ordering, and rotational and translational motional parameters using the 2D-FT-ESR spectral simulation theory and computer programs of Lee et al. (1994b), modified for NLLS analysis (Budil et al., 1996). These programs are based on the Stochastic-Liouville theory for time domain ESR that has been reviewed by Schneider and Freed (1989).

The rotational mobility of the spin-labeled molecules using the standard model is characterized by rotational diffusion constants, $R_\perp$ and $R_\parallel$, which represent the principal values of an axially symmetric rotational diffusion tensor. For 16-PC they represent rotational motion parallel and perpendicular to the preferred orientation of the long hydrocarbon chain of the lipid molecule. Actually, $R_\perp$ and $R_\parallel$ represent a simple approximation to the complex internal modes of motion of the chain as well as the overall motion (Ferrarini et al., 1989). The translational mobility is characterized by the Heisenberg exchange frequency, ω_{HE}, which measures the rate of bimolecular encounters of the spin-labeled molecules.

Lipid molecules in bilayers experience orienting potentials that restrict the amplitudes of the rotational motion. That is, the larger the orienting potential, the smaller will be the range of the orientations sampled by the motion. More precisely, the orienting potential, $U(\Omega)$, yields an orientational distribution of the molecules with respect to the local ordering axis of the membrane bilayer, known as the local director, corresponding to each bilayer segment in the vesicle. It is usually expressed as an expansion in generalized spherical harmonics,

$$-U/kT = c_0^2 D_{00}^2(\Omega) + c_2^2(D_{00}^2(\Omega) + D_{0-2}^2(\Omega)) + c_0^4 D_{00}^4(\Omega) + \cdots \qquad (2)$$

where $\Omega = (\alpha, \beta, \gamma)$ are the Euler angles between the molecular frame of the rotational diffusion tensor and the local director frame. The c_0^2, c_2^2, and c_0^4 are dimensionless potential energy coefficients, k is Boltzmann's constant, and T is the temperature. The commonly used order parameter S is defined by

$$S = \langle D_{00}^2 \rangle = \left\langle \frac{1}{2}(3\cos^2\beta - 1) \right\rangle = \int d\Omega \exp(-U/kT) D_{00}^2(\Omega) \Big/ \int d\Omega \exp(-U/kT), \qquad (3)$$

and another order parameter $S_2 = \langle D_{01}^2 + D_{0M-2}^2 \rangle$ is defined in a similar manner. It represents the deviation from axial symmetry of the molecular alignment relative to the local director.

For simulating the spectra from lipid vesicles, the MOMD model was incorporated. This means that different bilayer segments are randomly oriented with respect to the lab z axis, which is taken to be along the axis of the static magnetic field. Then the spectrum from the dispersion sample can be regarded as a superposition of the spectra from all fragments, which can be written as

$$S_{c\pm}^{MOMD} = \int S_{c\pm}(\psi)\sin\psi \, d\psi \qquad (4)$$

where $S_{c\pm}(\psi)$ is the ESR spectrum from a membrane fragment with ψ the angle of tilt of the normal to its bilayer relative to the lab z axis. The effects of MOMD on the 2D-ESR spectra are discussed in Lee et al. (1994b). We calculated spectra for 10 different values of ψ, and then averaged them over a unit sphere to produce a single MOMD spectrum.

The simulations also included effects of dead time in t_1 and t_2, which were fixed at experimentally measured values (50 ns along both t_1 and t_2). The effect of a finite pulse width may be regarded as a small correction to the dead time (i.e., a 5-ns pulse width versus 50-ns dead time, Crepeau et al., 1994).

The first step for a NLLS simulation was to choose reasonable starting values for $R_\perp$ $R_\parallel$, c_0^2, c_2^2, ω_{HE}, and Δ_G, where Δ_G is the additional Gaussian inhomogeneous width parameter. This essentially is the broadening arising from proton shfs, which modifies the unbroadened signal according to Gamliel and Freed (1990) and Lee et al. (1994b)

$$S_{c\pm}^{GIB} = S_{c\pm}\exp[-2\pi^2\Delta_G^2(t_1 \pm t_2)^2], \qquad (5)$$

where Δ is in frequency units. For all the NLLS fits reported in this work, the simulations were quite insensitive to $R_\parallel$, so instead of varying $R_\perp$ and $R_\parallel$ independently, we kept the ratio $R_\parallel/R_\perp$ fixed at 10 (Shin and Freed, 1989) and varied $\bar{R}$, where $\bar{R} = (R_\parallel R_\perp^2)^{1/3}$.

The S_{c+} and S_{c-} spectra were significantly different at all temperatures, the differences becoming more prominent as the temperature was lowered. At a given temperature their differences were greater for DPPC/GA samples than for DPPC samples. The S_{c+} and S_{c-} data were processed separately as discussed by Crepeau et al. (1994).

We found that inclusion of a diffusion tilt parameter, ϕ, improved the fits. The improvement was more noticeable for the S_{c-} fits than for the S_{c+} fits, consistent with the better resolution of the former. This angle ϕ represents the tilt of the magnetic tensor principal axis with respect to the principal axis of diffusion (Schneider and Freed, 1989; Ge and Freed, 1993). At the lower temperatures, (especially in the gel phase, i.e., <45°C) we could not satisfactorily fit the S_{c-} data without a $\phi \neq 40°$. We therefore processed all the data with a diffusion tilt. When ϕ was varied in the NLLS fits, we obtained an optimum value of 31 ± 2° over the entire range of temperatures. We thus performed separate fits with $\phi = 0°$ and $\phi = 31°$ for comparison, but we report herein the results for $\phi = 31°$. [As an example, at 50°C the rms deviation in the S_{c-} spectral fit was reduced by 11% for the pure DPPC and by 16% for the DPPC/GA samples when $\varphi = 31°$ was used instead of $\varphi = 0°$].

RESULTS

General observations: liquid crystalline phase

We first illustrate the enhanced spectral resolution of 2D ELDOR to the effects of adding GA to the DPPC membrane. In Figs. 2 and 3 we show the S_{c-} 2D spectra versus the cw spectra taken in the absence and in the presence of GA. These figures are for 80° and 45°C, respectively, and result from the 16-PC probe. The primary discernible effects in the cw spectra are the small derivative peak height changes that result from a change in linewidths when GA is added. The S_{c-} 2D spectra show a richer array of changing

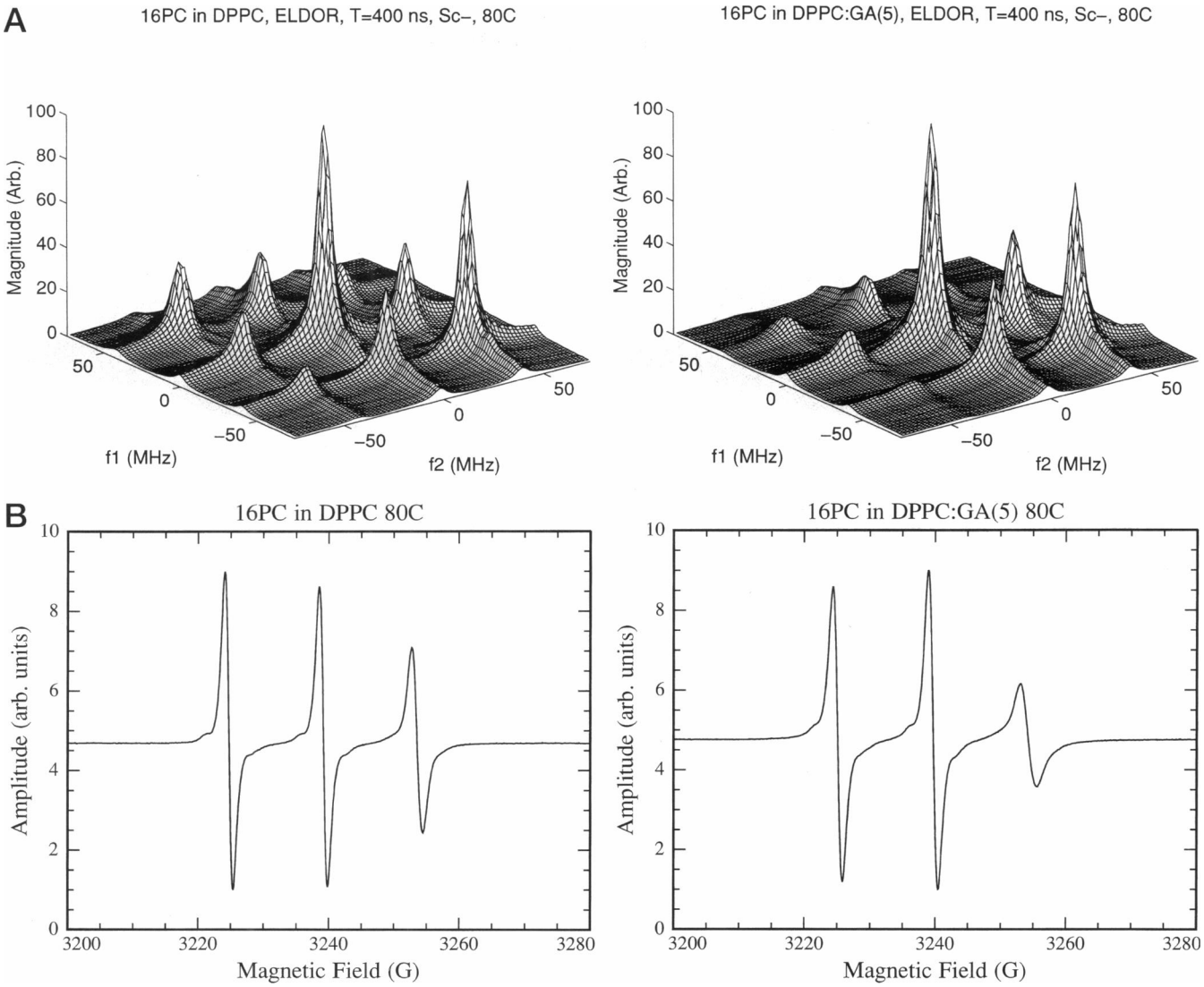

FIGURE 2 (*A*) A comparison of 2D-ELDOR S_{c-} spectra at 80°C with (*right*) and without (*left*) GA in DPPC for a mixing time of T_m = 400 ns. (*B*) Corresponding CW ESR spectra.

heights and shapes of the three autopeaks and the six crosspeaks. In addition, for 2D-ELDOR one may track the growth in the crosspeaks, as well as lineshape changes that occur by obtaining a series of S_{c-} spectra as a function of mixing time, T_m, as illustrated in Figs. 4-7 for pure DPPC and for DPPC/GA. Their behavior is markedly different in the presence of GA than in its absence.

Because the S_{c-} spectra yield spin-echo-like cancellation of inhomogeneous broadening, which occurs along the $t_1 = t_2$ axis in the time representation, (Lee et al., 1994b), they are found to be much sharper and better resolved than their S_{c+} counterparts. Thus we shall emphasize the results from fitting the S_{c-} spectra.

Spectral simulations

The best spectral fits are shown in Figs. 4–7 alongside the experimental spectra. Each series of 6–8 2D spectra obtained as a function of T_m have been fit with a single set of parameters. For purposes of presentation we have only shown three examples for each series. The best fit parameters to the S_{c-} data are given in Tables 1 and 2 for the case of a diffusion tilt, $\phi = 31°$. These results cover the six temperatures studied in the L_α phase from 45° to 80°C. They unequivocally demonstrate that the addition of GA to a 5:1 ratio of DPPC to GA leads to 1) a reduction in the rotational diffusion coefficient by a factor of ~3 over the whole temperature range; 2) a reduction in the Heisenberg exchange rate by a factor of 2–3 in the range of 60–80°C, and an $\omega_{HE} < 1 \times 10^6$ s^{-1} as an upper limit at 45–50°C; and 3) only a small increase in order parameter S by ~10–20%.

Thus the principal effect of the GA on the membrane is found to be one of substantially reducing the fluidity as monitored by both the rotational and translational diffusion with only a small increase in the ordering potential. (The

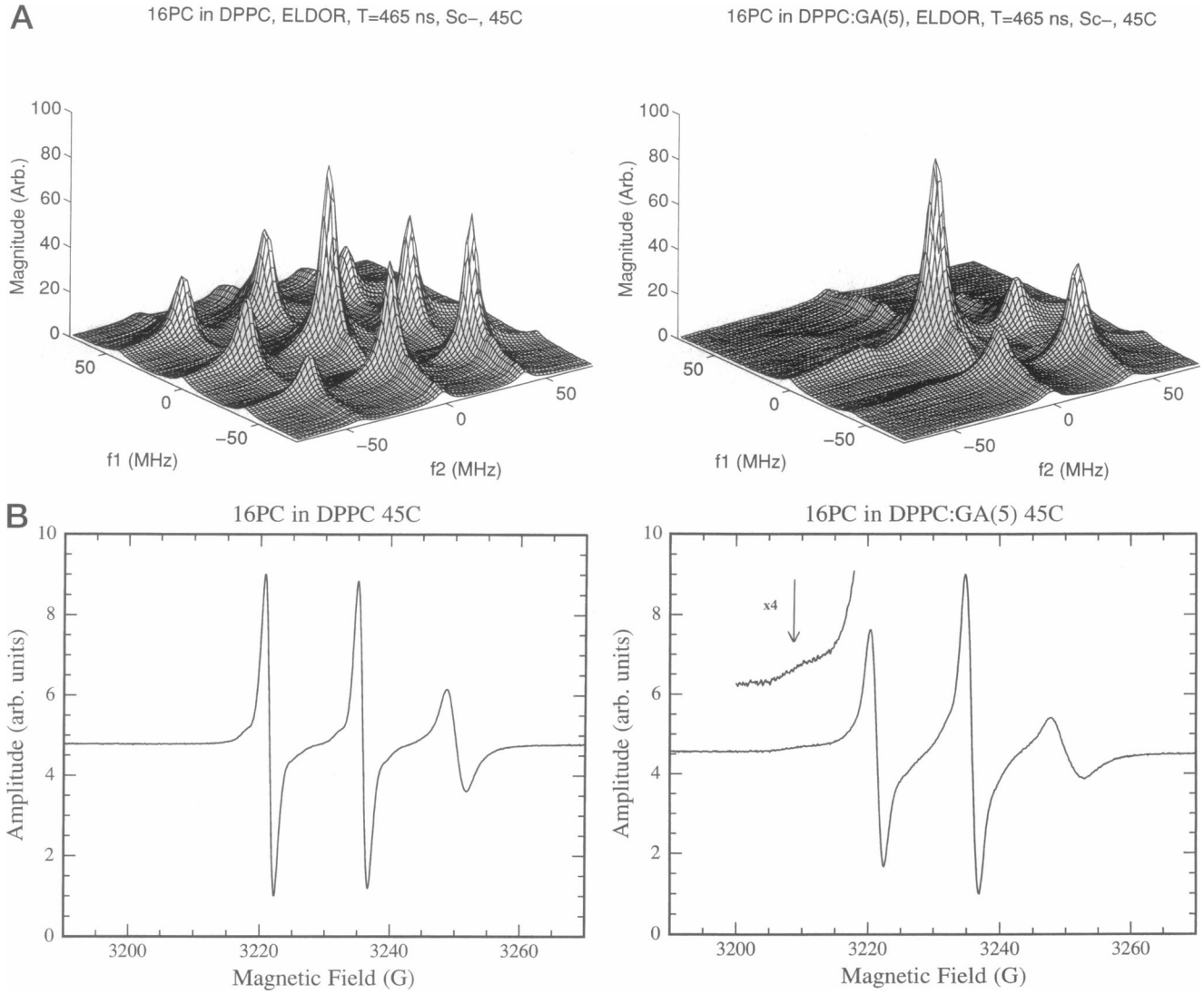

FIGURE 3 (*A*) A comparison of 2D-ELDOR S_{c-} spectra at 45°C with (*right*) and without (*left*) GA in DPPC for a mixing time of T_m = 465 ns. (*B*) Corresponding CW ESR spectra. Note the arrow pointing to signal from "immobilized" component (cf. text).

qualitative picture is not changed if the S_{c+} fits are used, but there is more uncertainty in the results).

When the spectra are fit to the case of no diffusion tilt, i.e., $\phi = 0°$, generally poorer fits are obtained as described above. It was also no longer possible to extract an ω_{HE} in the DPPC/GA cases nor an S in most cases. However, the trends in $R_\perp$ and S with addition of GA and with temperature are about the same. However, the absence of tilt leads to a systematic increase in the fitted values of $R_\perp$ by about a factor of 2 and a systematic decrease in S by nearly a factor of 2, as one expects (Ge and Freed, 1993).

The electron-spin-lattice relaxation times, T_{1e}, that have been extracted from the 2D-ESR spectra versus T_m (Crepeau et al., 1994; Lee et al., 1994b) show substantial decrease with increasing temperature as expected from a spin-rotational-type mechanism (Hwang et al., 1975). The somewhat shorter T_{1e} in the presence of the GA is, however, opposite to the trend expected given $R_\perp$ is reduced by the addition of GA (Hwang et al., 1975). [Note that the T_{1e} values were fitted to the sets of 2D spectra only after fitting the other parameters in Tables 1 and 2, so they can be corrupted by deficiencies in the models used, cf. below].

Gel phase: observations and simulations

We turn now to the gel phase results. Only the 2D spectra at 35°C were studied in detail, although spectra at 25°C were also obtained. Typical gel-phase 2D spectra are shown in Figs. 8 and 9. The gel-phase 2D spectra are broader and less resolved than those from the L_α phase. The S/N is much poorer for the S_{c+} spectra than for the S_{c-} spectra, since the former decay more rapidly during the spectrometer dead time (~50 ns). This difference manifests itself as a reduced signal for the S_{c+} spectrum in the frequency domain as shown in Fig. 9, where both the S_{c+} and S_{c-} signals obtained at T_m = 165 ns are plotted to the same scale. Thus we

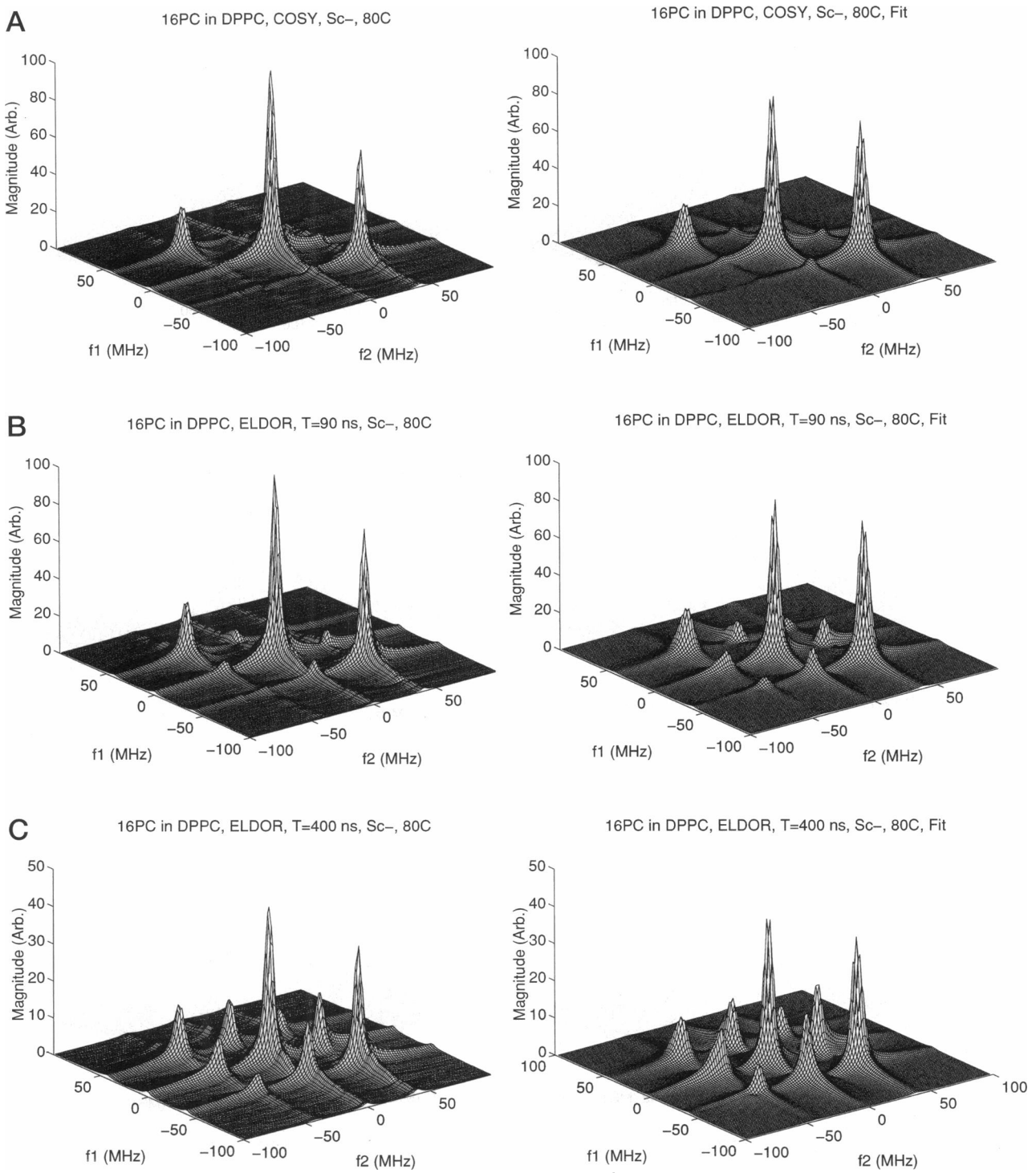

FIGURE 4 A comparison of experimental 2D-ELDOR S_{c-} (*left*) and simulated (*right*) spectra of 16-PC in DPPC at 80°C as a function of mixing time: (*A*) T_m = 0 ns (COSY); (*B*) T_m = 90 ns; and (*C*) T_m = 400 ns. (Parameters in Table 1).

again concentrate on the S_{c-} signals. The S_{c-} gel-phase spectra showed rather substantial discrepancies between experiment and best simulations, (e.g., Fig. 8). Also, the generally reduced resolution due to the broader lines manifests itself by less obvious spectral changes arising from addition of GA (but see below). Our best fits to the S_{c-} spectra yielded the results in Table 3. When we compare the S_{c-} results in Table 3 with those in Tables 1 and 2, we find a substantial reduction in $R_\perp$ in the gel phase by a factor of ~5 for pure DPPC and a factor of ~2.5 for DPPC/GA in going from 45°C and 35°C. Meanwhile, S more than doubles in both cases. These two changes of decreased $R_\perp$ and

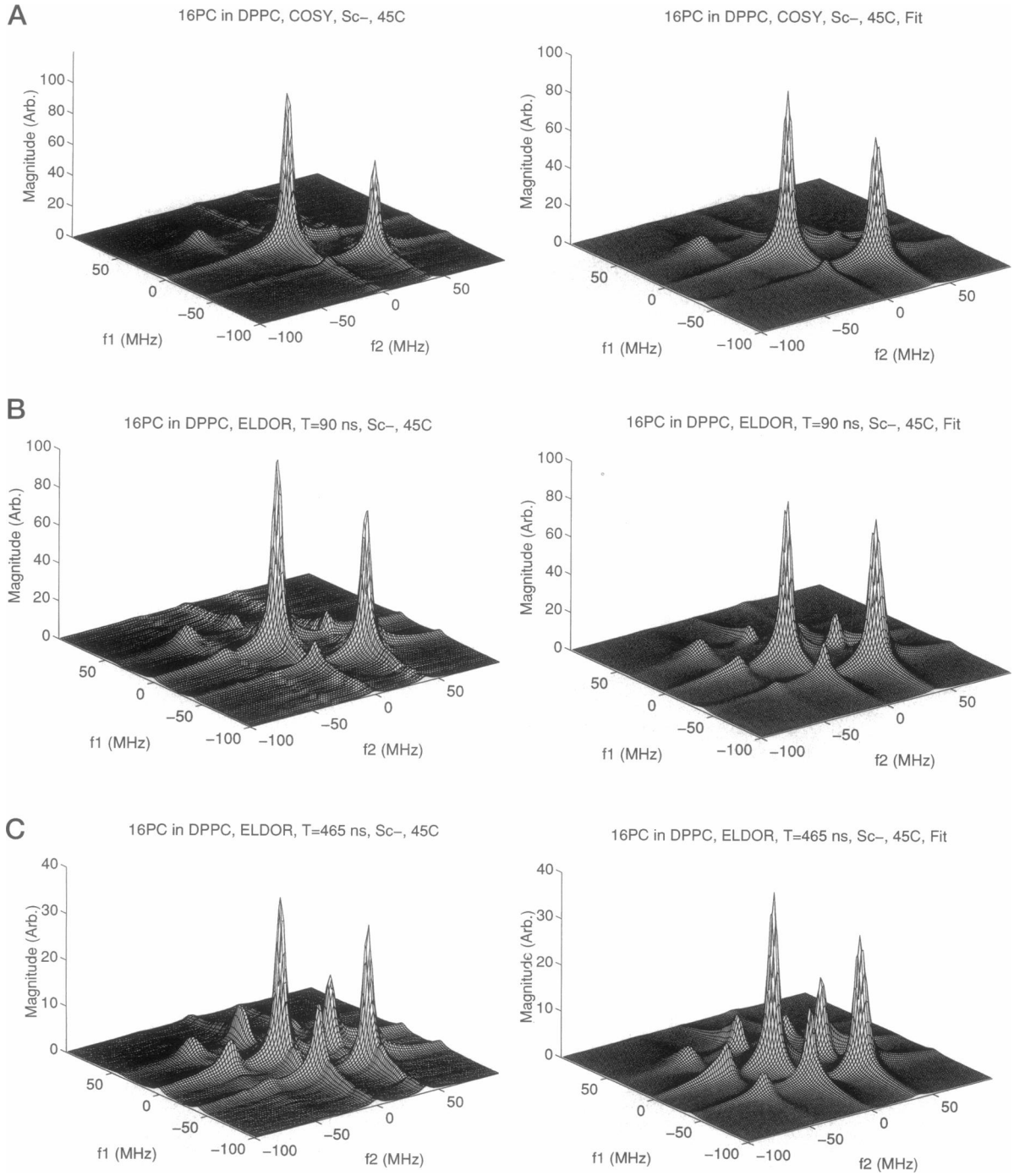

FIGURE 5 A comparison of experimental 2D-ELDOR S_{c-} (*left*) and simulated (*right*) spectra of 16-PC in DPPC at 45°C as a function of mixing time: (*A*) T_m = 0 ns (COSY); (*B*) T_m = 90 ns; and (*C*) T_m = 465 ns. (Parameters in Table 1).

increased S are the source of the large changes in 2D spectral features in going from the L_α to gel phase, and again emphasize the sensitivity of 2D-ESR spectra to dynamics and ordering. However, given that the values for $R_\perp$ and S are more nearly equal for pure DPPC and DPPC/GA in the gel phase than in the L_α phase, this is an additional reason why their 2D spectra do not show very large differences. Finally, we emphasize that the use of no diffusion tilt, i.e., $\phi = 0°$, leads to much poorer fits.

Absence of spectral features associated with "immobilized" component

In one key respect we observe that there are details in the cw spectra that are not manifest in the 2D-ELDOR spectra. This is, for example, clearly seen in Fig. 3 *b*. There is a second component that appears in the 45°C cw-ESR spectrum with the GA present. This is, of course, fully consistent with the observations of many workers (Devaux and Seignenret,

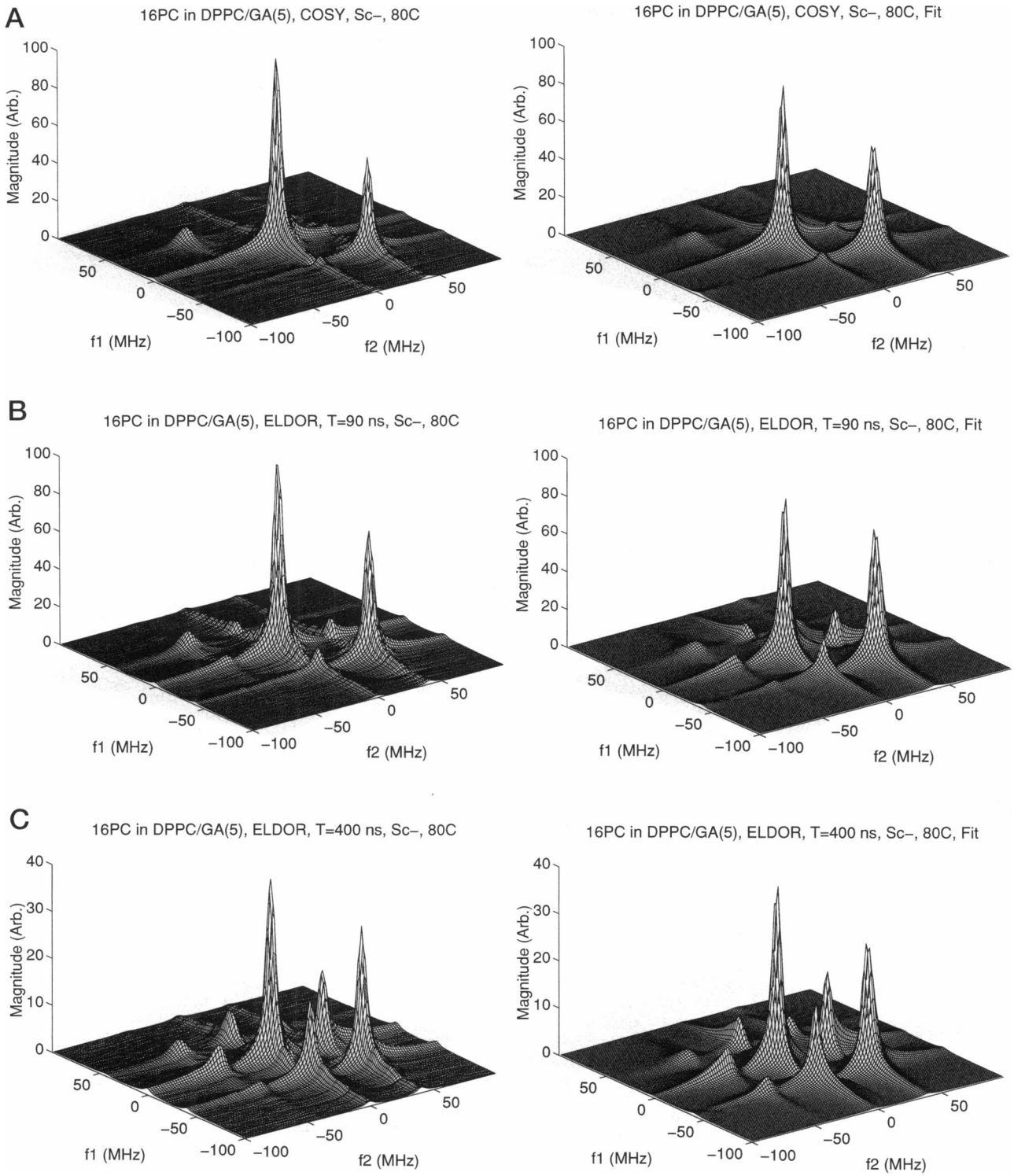

FIGURE 6 A comparison of experimental 2D-ELDOR S_{c-} (*left*) and simulated (*right*) spectra of 16-PC in DPPC/GA at 80°C as a function of mixing time: (*A*) T_m = 0 ns (COSY); (*B*) T_m = 90 ns; and (*C*) T_m = 400 ns. (Parameters in Table 2).

1985; Marsh, 1985, 1989; Ge and Freed, 1993). In an attempt to determine why no such spectral features appear in the 2D-ELDOR, and what their absence implies about DPPC/GA interactions, we utilized the following approach, based on the Ge-Freed (GF) analysis.

GF provided extensive simulations for their cw-ESR spectra that are very similar to those shown in Figs. 1 and 2, utilizing several proposed models. Most relevantly, they studied a model made up of lipid components that differed only in their motional rates (their model 1 found in their

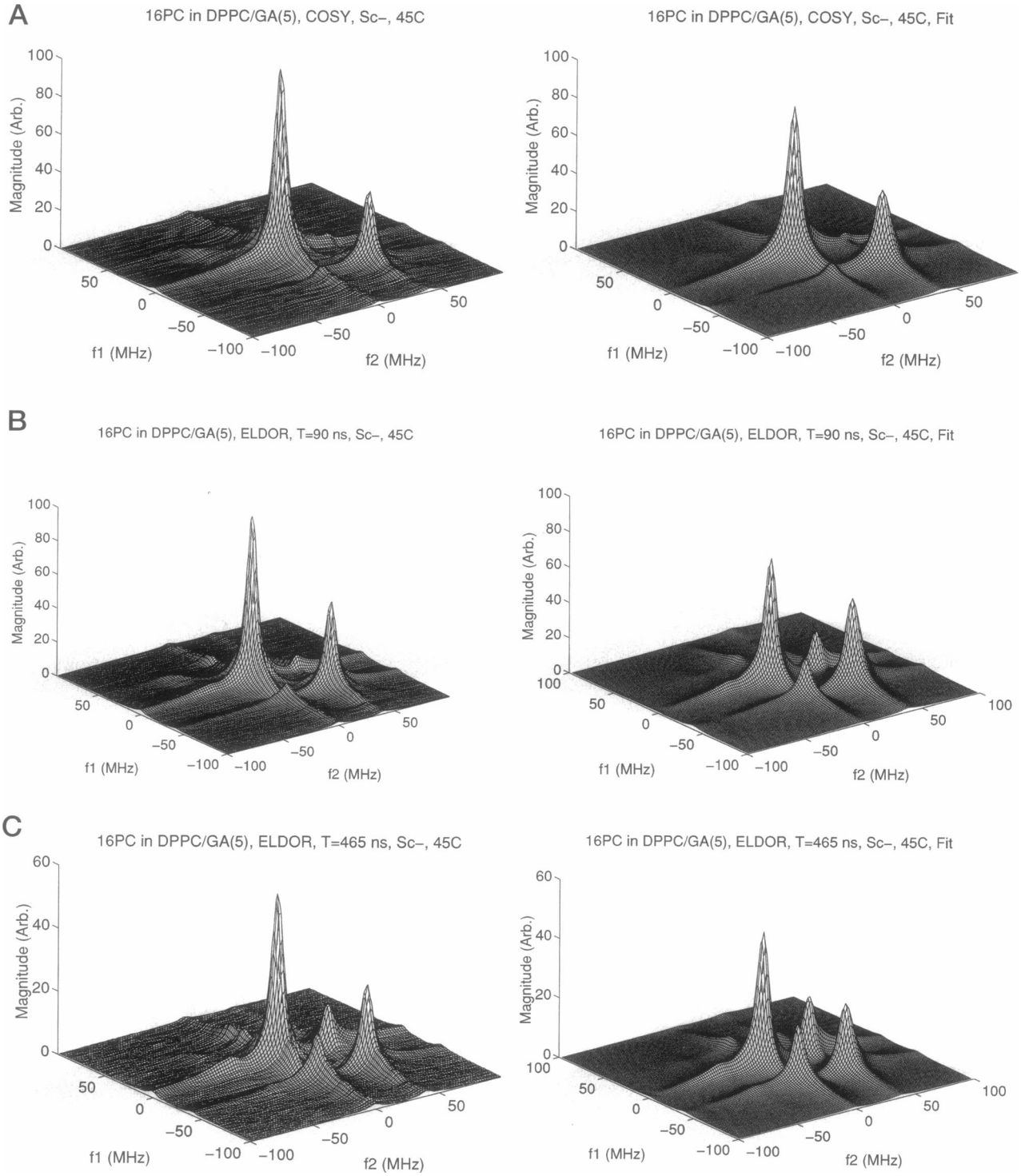

FIGURE 7 A comparison of experimental 2D-ELDOR S_{c-} (*left*) and simulated (*right*) spectra of 16-PC in DPPC/GA at 45°C as a function of mixing time: (*A*) T_m = 0 ns (COSY); (*B*) T_m = 90 ns; and (*C*) T_m = 465 ns. (Parameters in Table 2).

Table 5) and another model in which they differed primarily in their order parameters (their model 3 found in their Table 3). We used these two models to simulate the 2D-ELDOR spectra, to address which, if either, would be consistent with our observations. In Fig. 10 we show the simulated 2D-ELDOR spectra for the four relevant components used by GF to fit with model 3. Their pattern varies dramatically, primarily due to the changes in ordering.

One sees that as the ordering increases there is a large enhancement of the MOMD effect on 2D-FT-ESR spectra; namely, an increased broadening of the autopeaks along the $f_1 = f_2$ diagonal. One also notices a sharpening of the

TABLE 1 16-PC in DPPC, S_{c-}

Temp. (°C)	Δ_G	$R_\perp(10^8 s^{-1})$	$\omega_{HE}(10^6 s^{-1})$	$C_{20}(kT)^{-1}$	$C_{22}(kT)^{-1}$	S	S_2	$T_{1,e}(10^{-6} s^{-1})$
45	0.51	2.4	5.3	0.859	−0.164	0.186	−0.049	12.7
50	0.52	2.9	5.1	0.748	−0.139	0.161	−0.042	10.0
60	0.49	3.9	7.4	0.705	—*	0.151	—*	3.4
70	0.56	5.3	7.4	0.578	—*	0.123	—*	1.28
80	0.56	6.5	7.6	0.563	—*	0.119	—*	1.01

Magnetic parameters: $A_{xx} = A_{yy} = 5.0$ G, $A_{zz} = 33.0$ G, $g_{xx} = 2.0089$, $g_{yy} = 2.0058$, $g_{zz} = 2.0021$ (Ge and Freed, 1993). Average percent errors in simulation parameters: Δ_G (10%), $R_\perp$ (5%), ω_{HE} (10%), S (2%), S_2 (2%), $T_{1,e}$ (20%). Diffusion tilt: $\varphi = 31°$.
*C_{22} very small, so kept fixed at 0.

spectra perpendicular to this direction with increased ordering. This is due to the decrease in the range of orientations as the motion becomes more restricted. (The modest changes in $R_\perp$ used have only a secondary effect). As a result of spectral broadening in one direction and sharpening in an orthogonal one, the amplitudes of these 2D spectra remain comparable. Thus, when they are superimposed according to the statistical weights of GF, a composite spectrum, shown in Fig. 11, is obtained. In fact, it is the spectrum of pure component 5 that reasonably resembles our experimental results for pure DPPC at 45°C (cf. Fig. 5). Small differences are due to the somewhat different parameters used by GF for this component than the optimum values. When we compare Fig. 7 for the case of DPPC/GA at 45°C with the simulation of Fig. 11, we see that it bears very little resemblance to the experiment. Thus the possibility of primarily a substantial increase in membrane ordering, either for a single component or by the appearance of new components, upon addition of GA appears to be ruled out.

We turn now to simulations of 2D-ELDOR spectra based upon model 1 of GF. Here we show the five components that they considered, wherein the motional rates are decreased over a range of more than an order of magnitude (cf. Fig.12). These are a different set of cases than for model 3. Nevertheless, GF found that superposition of their cw-ESR spectra do approximate, though not as well, the cw-ESR spectra obtained from DPPC/GA mixtures. The combined 2D spectrum, shown in Fig. 13, is seen to be practically the same as that of component 1 in Fig. 12. The reason for this should be clear from Fig. 12; the amplitudes of the 2D peaks fall off dramatically as the rotational rate, $R_\perp$, drops off. One expects the amplitudes to decrease as the line-broadening increases due to the slower motion. However, the drop by almost a factor of 400, shown in Fig. 12, has been amplified by the effect of the spectrometer dead time of 50 ns. During that dead time those components with the shorter T_2 values (i.e., the broader homogeneous widths) will exponentially decay away much more quickly. We can conclude from Figs. 12 and 13, and other simulations we performed, that any components in the experimental 2D spectrum characterized by a $2 \times 10^6 \leq R_\perp \leq 6 \times 10^7\ s^{-1}$ and low ordering (i.e., $S < 0.10$) would most likely not be observable in the experimental spectra given their low 2D amplitudes and available S/N.

[Added in proof: In a new cw-ESR study, we do find that the second (or slow) component is adequately fit with $R_\perp$ in this range, and the 2D-ELDOR spectrum predicted (using the cw-ESR fitting parameters) is virtually unaffected by the presence of this slow component, consistent with observation. However, very small effects on the 2D-ELDOR spectrum are predicted, and we find that such effects might be barely discernable in the experiments].

Variation of apparent T_2 values with mixing time

We turn next to the observation, first reported by Crepeau et al. (1994), that the apparent homogeneous linewidths T_2^{-1} are observed to increase with mixing time, T_m, as described in the Methods section. We show in Fig. 14 plots of $(T_2^{-1})_{app}$ versus mixing time for 70°C and 45°C and the least squares fits to Eq. (1) for both pure DPPC and DPPC/GA. The values for the Δ_{LW} parameter and τ_c are collected in Table 4. Note that Δ_{LW} shows only a small 10% decrease with decreasing temperature and no significant difference between pure DPPC and DPPC/GA. However, τ_c decreases substantially with decrease in temperature by almost a factor of 2, with only a small increase due to addition of GA.

TABLE 2 16-PC in DPPC/GA 5:1, S_{c-}

Temp. (°C)	Δ_G	$R_\perp(10^8 s^{-1})$	$\omega_{HE}(10^6 s^{-1})$	$C_{20}(kT)^{-1}$	$C_{22}(kT)^{-1}$	S	S_2	$T_{1,e}(10^{-6} s^{-1})$
45	0.50	0.76	—*	1.003	−0.231	0.218	−0.064	10.5
50	0.44	0.98	—*	0.887	−0.264	0.190	−0.077	2.7
60	0.47	1.47	2.5	0.706	−0.031	0.153	−0.010	1.38
70	0.47	1.80	3.7	0.726	−0.008	0.157	−0.003	0.93
80	0.50	2.48	4.5	0.646	−0.078	0.139	−0.025	—

Magnetic parameters: $A_{xx} = A_{yy} = 5.0$ G, $A_{zz} = 33.7$ G, $g_{xx} = 2.00867$, $g_{yy} = 2.00591$, $g_{zz} = 2.00212$ (Earle et al., 1994). Average percent errors in simulation parameters: Δ_G (10%), $R_\perp$ (5%), ω_{HE} (10%), S (2%), S_2 (2%), $T_{1,e}$ (20%). Diffusion tilt: $\varphi = 31°$.
*ω_{HE} very small.

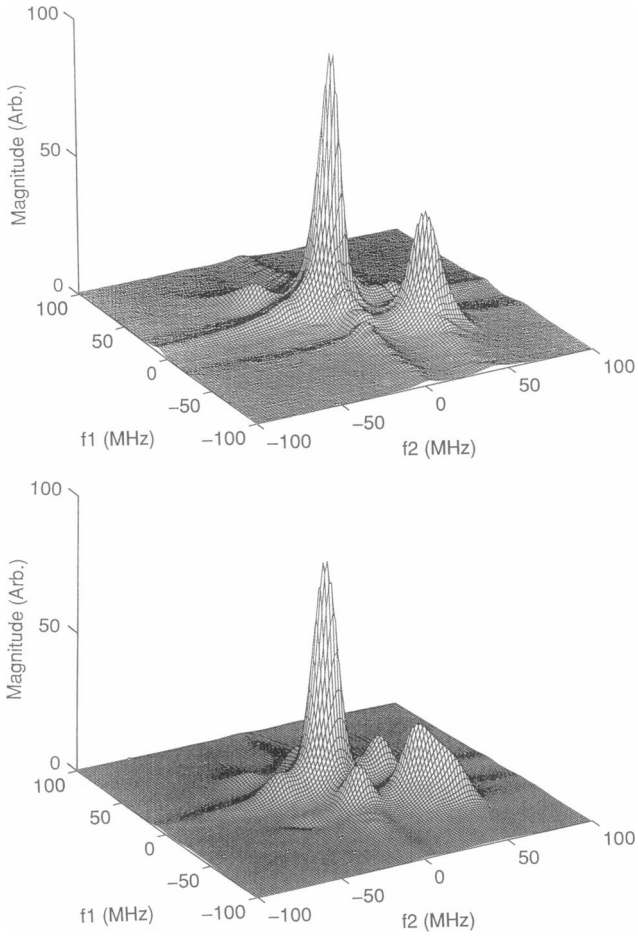

FIGURE 8 2D-ELDOR S_{c-} experimental (*top*) and simulated (*bottom*) spectra for 16-PC in DPPC in the gel phase at 35°C with T_m = 165 ns (Parameters in Table 3).

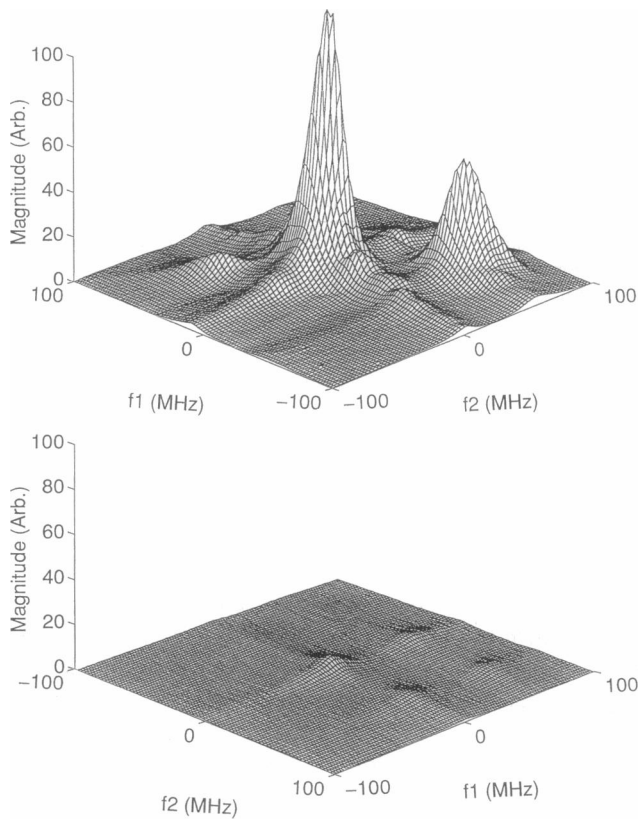

FIGURE 9 A comparison of experimental 2D-ELDOR S_{c-} (*top*) and S_{c+} (*bottom*) T_m = 165 ns spectra for 16-PC in DPPC/GA at 35°C (gel phase).

Such a decrease for a rate process might at first appear surprising, but there are other known examples, as we discuss below.

DISCUSSION

2D-FT-ESR and heterogeneity of lipids

The greater resolution of 2D-ELDOR, (especially when studied as a function of T_m) versus cw-ESR to ordering and dynamics has allowed an unequivocal characterization of the effects on the bulk lipids of addition of GA to DPPC membrane vesicles in the L_α phase. There is a significant reduction in both rotational and translational diffusion rates of the bulk lipids, but only a small increase in their ordering. However, indications of a second immobilized component, upon addition on GA, that are seen in this and much past work using cw-ESR are not manifest in the 2D-ELDOR results. Our analysis of this observation in the Results section leads us to conclude that such an "immobilized component" is most likely one characterized by a reduced motional rate, but not so slow that it approaches the rigid limit, nor can it be one that is characterized primarily by substantially increased ordering.

This conclusion is to be contrasted with that of GF, from their simulations of the cw-ESR spectra in terms of admixing several components, wherein model 3 gave the best fits, and model 1 was less satisfactory. Their introduction of a heterogeneity of lipids resulting from the addition of GA is a point of view that was supported by the results from fluorescence lifetime decay (Williams and Stubbs, 1988) and FTIR (Casal and McElhaney, 1990), although it was pointed out that these techniques correspond to much shorter time scales than ESR experiments. GF do, of course, point out the very limited resolution of MOMD-ESR. Furthermore, although they performed extensive simulations, they did not have available at that time the newest least-squares algorithms that enable fitting several components (Ge et al., 1994; Budil et al., 1996), so their analysis was more in the spirit of model simulations, wherein components were selected in a trial-and-error manner.

Those conclusions of GF were somewhat in contrast to the model, introduced by Jost et al. (1973) and further developed by others (Knowles et al., 1979; Watts et al., 1979; Marsh and Watts, 1982; Marsh, 1989; Devaux and Seignenret, 1985), that was based on the observations of the "two-component-like" ESR spectra from spin-labeled lipids in various protein-containing membranes. The model of

TABLE 3 16-PC in DPPC/DPPC/GA 5:1, S gel phase, 35°C

Sample	Δ_G	$R_\perp(10^8 s^{-1})$	$C_{20}(kT)^{-1}$	$C_{22}(kT)^{-1}$	S	S_2
DPPC	1.34	0.46	2.32	1.07	0.454	0.158
DPPC/GA	2.01	0.32	2.67	−1.25	0.504	−0.155

Magnetic parameters, average percent errors, and diffusion tilt are the same as in Table 2.

these other authors is that the rotational motion of a lipid in the immediate vicinity of the protein (the so-called boundary lipid) is immobilized. That is, the $R_\perp \leq 3$ μs (Marsh, 1989) which is approaching the rigid limit on the ESR time scale. Our present analysis is consistent with an appreciable slowing down of the motion of the boundary lipid, but not necessarily much slower than ~1 μs. The model that GF favored (i.e., model 3) is, as we have seen, one with increased order parameters, but not large changes in $R_\perp$. That such different possibilities can be attributed to the same cw-ESR spectra in the case of MOMD is a clear demonstration of their very limited resolution. That is, increasing

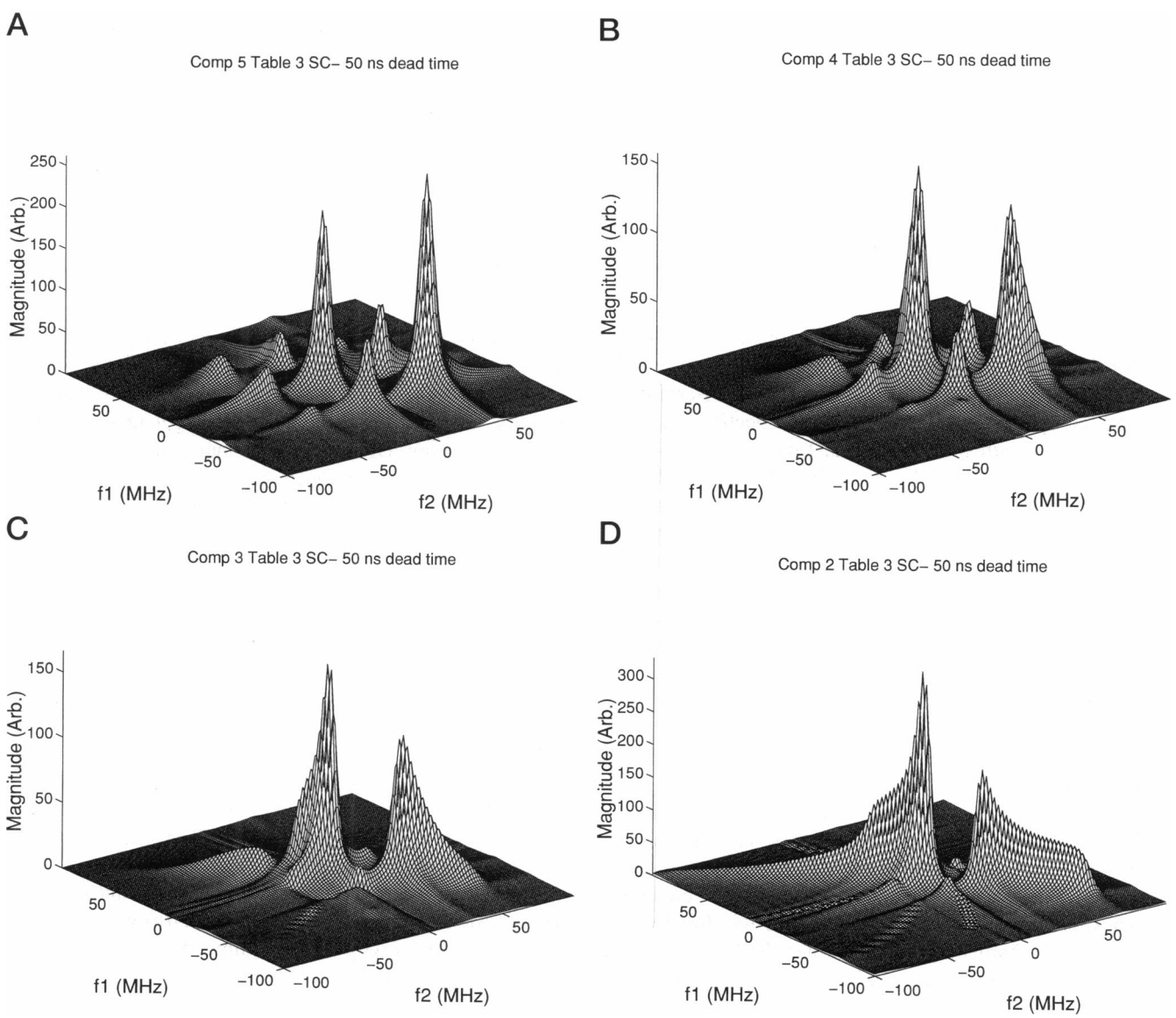

FIGURE 10 Simulation of components for the 2D-ELDOR spectra of 16-PC in DPPC/GA for a 5:1 ratio at 45°C according to the model of Ge and Freed based on increased ordering: (*A*) component 5: $R_\perp = 4.4 \times 10^8\ s^{-1}$, $R_\parallel = 6.7 \times 10^8\ s^{-1}$, $C_{20} = 0.5$, $C_{22} = -0.4$, $S = 0.10$; (*B*) component 4: $R_\perp = 3.5 \times 10^8\ s^{-1}$, $R_\parallel = 8.4 \times 10^8\ s^{-1}$, $C_{20} = 1.2$, $C_{22} = -0.4$, $C_{40} = 0.5$, $C_{42} = 0.2$, $S = 0.30$; (*C*) component 3: $R_\perp = 2.9 \times 10^8\ s^{-1}$, $R_\parallel = 10.0 \times 10^8\ s^{-1}$, $C_{20} = 2.0$, $C_{22} = -0.5$, $C_{40} = 1.2$, $C_{42} = 0.3$, $S = 0.56$; (*D*) component 2: $R_\perp = 2.4 \times 10^8\ s^{-1}$, $R_\parallel = 10.0 \times 10^8\ s^{-1}$, $C_{20} = 3.2$, $C_{22} = -0.5$, $C_{40} = 1.5$, $C_{42} = 0.5$, $S = 0.78$. In all cases a $\Delta_G = 0.6$ G was used with a $\tau_d = 50$ ns and a $T_m = 365$ ns.

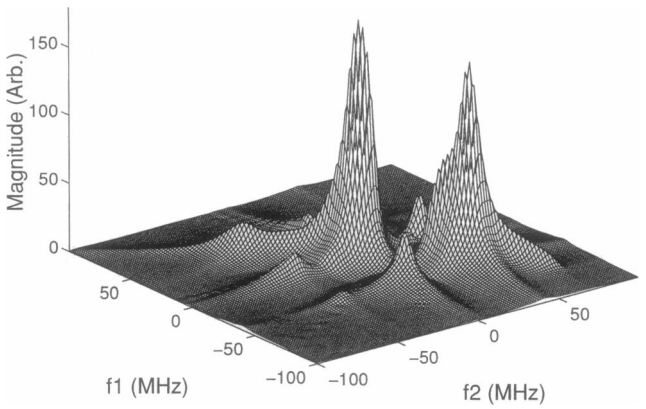

FIGURE 11 The composite 2D-ELDOR spectrum from the four components shown in Fig. 10, weighted as follows: components 5, 4, 3, and 2 are 38%, 7%, 36%, and 19%, respectively, to correspond to the model of Ge and Freed.

the ordering has somewhat similar effects to slowing the motional rates on the MOMD spectra. Subtle details could thus be fit with different types of admixtures of different components.

As was clear from our analysis based on Figs. 10–13, the finite spectrometer dead times will lead to a discrimination of component spectra with longer T_2 values. Thus future technical developments to reduce the dead time would be desirable, since they would enable components with slower motional rates to be observed. Such developments would permit a fuller utilization of 2D-ELDOR to discriminate discrete components. That is, after 2D spectra will have been collected with minimum dead time, one may artificially increase dead time (by discarding the data at shorter times) and observe how the 2D-ELDOR spectra change. The separability of two component spectra, with a substantial difference in their T_2 values, was previously demonstrated in another context for the earlier field-swept 2D methods by Millhauser et al. (1987). Such "T_2 discrimination" would provide another "dimension" to the spectral analyses.

Disordering versus hardening effects from addition of GA

Tanaka and Freed (1985), in their work on oriented lipid multilayers containing GA, distinguish two competing effects in the lipid-GA interaction, a disordering effect and a hardening effect. The disordering effect is when the presence of GA induces a disordering of the lipids either by reducing ordering or by randomization of the direction of alignment. The hardening effect is when the GA molecules make the membranes more solid, resulting in increased order and decreased rotational rates. They suggested that the disordering feature is dominant under conditions of low fluidity, with the hardening feature being dominant when there is high fluidity. Ge et al. (1994) concluded that well-aligned samples, even with appreciable water content (20 wt %), are still characterized by the disordering effect of GA, whereas vesicles in excess water are characterized by the hardening feature. Our present experiments on vesicles in a small excess of water show the hardening feature in terms of the decreased rotational rates, but only a small 10–20% increase in ordering. This may not be unreasonable given that for 16-PC there is considerable free volume at the end of the chain where the spin label is located. Ge et al. (1994) did find that addition of the protein bacteriorhodopsin to aligned membranes hardly affected the ordering of 16-PC, but did reduce its $R_\perp$ consistent with the present study on addition of GA. However, CSL (cholestane) showed a significant reduction in ordering under the same conditions. Also, we note that other workers, for example using ^{2}H-NMR (Rice and Oldfield, 1979), solid-state NMR (Cornell et al., 1988), Raman (Short et al., 1987), and FTIR (Lee et al., 1984) found that low GA concentrations increase the ordering of the lipid bilayers and high GA concentrations decrease their ordering. It is not unreasonable that at the 5:1 lipid to GA ratio used in the present study there is a balance of these two effects. One would need to extend the present 2D-FT-ESR experiments to study a range of lipid/GA ratios, and also a range of sites labeled along the chain (Lee et al., 1994a).

Gel phase and sensitivity of 2D-FT-ESR to motional model

We turn now to a discussion of the gel phase. As is well known, this is a more viscous and more highly ordered phase. We found (cf. Results section) that the change in fluidity, in going from the L_α to the gel phase, is more drastic for pure DPPC vesicles than for the DPPC/GA vesicles, although the ordering increases by about the same amount. These are significant observations, but we wish here to emphasize both the very large 2D spectral changes in going from the L_α phase S_{c-} spectra at 45°C (cf. Figs. 5 and 7) to the gel phase S_{c-} spectra at 35°C (cf. Figs. 8 and 9), and the greater difficulty in fitting the gel phase spectra. Although these are broader spectra, there are no unusual features that we would attribute to an admixture of different components. In fact, it is our best-fit simulations that display the more unusual, MOMD-like features even for pure DPPC (cf. Fig. 8 *bottom*). We wish to suggest that the imperfect fits are a manifestation of the use of a dynamic model that is oversimplified, and the enhanced resolution to ordering and dynamics provided by 2D-FT-ESR amplifies this fact.

The dynamic model utilized in this work and most previous ESR studies is that of anisotropic Brownian reorientation in a macroscopically aligning potential (Schneider and Freed, 1989). It does not distinguish between the overall lipid motions and the complex internal chain dynamics. There have been recent efforts to include an appropriately detailed model into the analysis of ESR lineshapes (Cassol et al., 1993, 1997), but a more approximate approach appears to be useful for the NLLS analysis of 2D-ELDOR spectra (Sastry et al., 1996a, b; Xu et al., 1996). In the study

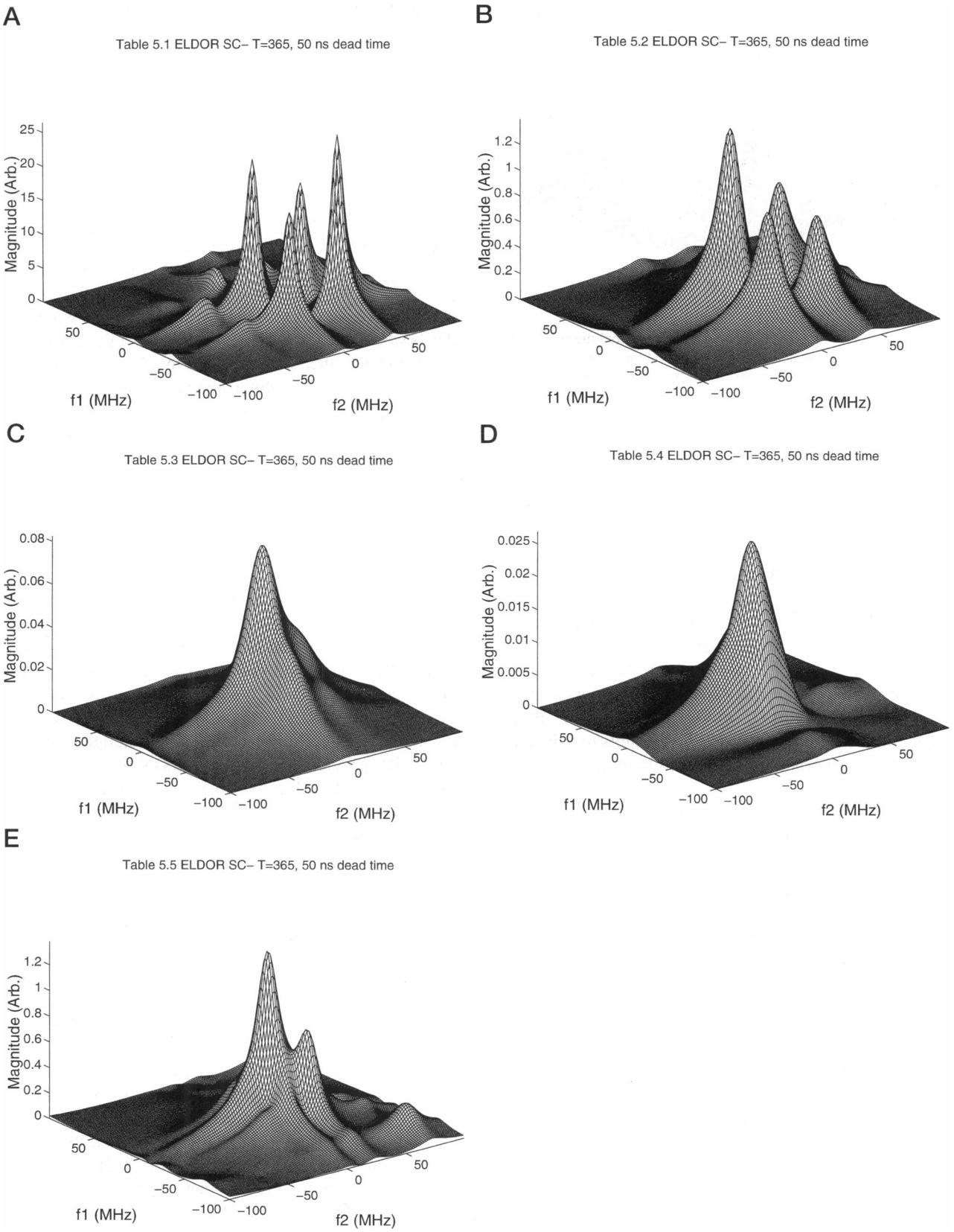

FIGURE 12 Simulation of components for the 2D-ELDOR spectra of 16-PC in DPPC/GA assuming decreased fluidity, according to Ge and Freed: (*A*) component 1: $R_\perp = 2.0 \times 10^8\ s^{-1}$, $R_\parallel = 5.6 \times 10^8\ s^{-1}$; (*B*) component 2: $R_\perp = 0.8 \times 10^8\ s^{-1}$, $R_\parallel = 5.6 \times 10^8\ s^{-1}$; (*C*) component 3: $R_\perp = 0.4 \times 10^8\ s^{-1}$, $R_\parallel = 5.6 \times 10^8\ s^{-1}$; (*D*) component 4: $R_\perp = 0.2 \times 10^8\ s^{-1}$, $R_\parallel = 4.0 \times 10^8\ s^{-1}$; (*E*) component 5: $R_\perp = 0.06 \times 10^8\ s^{-1}$, $R_\parallel = 1.0 \times 10^8\ s^{-1}$. In all cases $C_{20} = 0.33$ and $C_{22} = -0.38$ giving $S = 0.06$. Also, $\Delta_G = 0.6$ G was used with a $\tau_d = 50$ ns and a $T_m = 365$ ns.

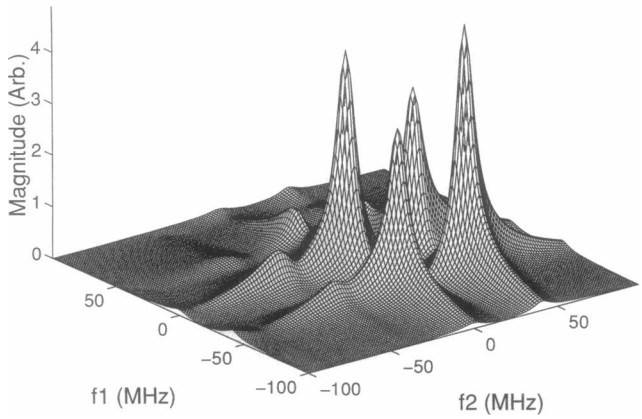

FIGURE 13 The composite 2D-ELDOR spectrum from the five components shown in Fig. 12, weighted as follows: components 1, 2, 3, 4, and 5 are 18%, 16%, 46%, 15%, and 5%, respectively, to correspond to the choice of Ge and Freed.

by Xu et al., on an end-chain-labeled polymer the internal chain dynamics experienced by the end-chain is specified by an effective axial rotational diffusion tensor, whereas the backbone structure of the polymer to which the nitroxide is attached, as well as any effects on the end-label from adjacent molecules, constitute a "cage" with a slower relaxation rate. They found that the use of this "dynamic cage" model significantly improved their fits to the experimental 2D-FT-ESR spectra. Indeed we do note some general similarities between Fig. 8 *a* and experimental results of Xu et al. (cf. Fig. 9 of that work). Thus, we would wish to address the challenge of fitting our 2D-FT-ESR results to a dynamic cage model appropriate to lipid membranes, in a future study.

We are inclined to interpret the significant discrepancies between simulation and experiment in the gel phase to be indicative of the need to use a dynamic model wherein both internal modes of motion and overall motion are explicitly included. One might expect that in the more viscous gel phase there will be a slowing down of the internal modes of motion such that there will be more appreciable line broadening and spin relaxation from this. (In fact, the significantly improved fits we achieved in the present work with a diffusion tilt angle of $\phi = 31°$, especially in the gel phase, is most likely a symptom of the need for a better model, rather than indicating this as the correct value). Although it is probably more important to use a more complete (e.g., "dynamic cage") model in fitting gel phase spectra, we do note systematic, but smaller, discrepancies in the fits to the L_α-phase shown in Figs. 4–7. These discrepancies show up in following our procedure of simultaneously optimizing a set of S_{c-} spectra obtained over a range of mixing times. (Individual 2D spectra can be better fit separately, but they each require somewhat different fitting parameters). These discrepancies are of the type that were found in the 2D-ELDOR study of spin probes in an oriented liquid crystal by Sastry et al. (1996a, b), which they fit to a simplified form of the dynamic cage model. In the future, the ability to distinguish the respective roles played by the internal chain dynamics versus the overall lipid motion should enable one to more precisely learn about the effects of added peptide or protein on the dynamic structure of membranes.

2D-FT-ESR and slow collective dynamics

We turn now to the slow process, which leads to the apparent increase in homogeneous T_2 as a function of mixing time, T_m. We have already considered the relatively fast processes of internal and overall motions of the lipids. An important slow process that has been clearly shown to affect the NMR T_1 and T_2 relaxation in lipid bilayers is that of order director fluctuations, which involves a collective motion of many phospholipid chains in the bilayer (Brown, 1982; Marqusee et al., 1984; Rommel et al., 1988; Watnick et al., 1990; Stohrer et al., 1991). These low-amplitude collective types of processes were shown to be too slow to affect ESR T_1 and T_2 relaxation given the faster time scale of the ESR experiment over that of the NMR experiment (Polnaszek and Freed, 1975; Freed, 1977; Freed et al., 1994). Instead, the ESR time scale is able to "freeze-out" such a process yielding a very small inhomogeneous contribution to the line broadening. In the 2D-ELDOR experiment one thus could have an opportunity to watch in real time (i.e., as a function of T_m) these order director fluctuations (ODF), provided one has very good spectral resolution. The spectral resolution provided by our 2D-ELDOR experiments is given by the homogeneous $T_2^{-1} \approx 1 \times 10^7$ s^{-1} (or 0.57 G), and the additional inhomogeneous broadening (IB) provided by the slow process is $\Delta_{LW} \approx 4 \times 10^6$ (or 0.23 G) (cf. Table 4). Note that such an additional IB would not even be observable in a cw-ESR experiment on membrane vesicles, because it would be buried in the MOMD effect, but it would contribute, as a source of "mosaicity" in the case of oriented multilayers. One can make estimates of the mean square amplitude of the director fluctuations, $\langle\theta_0^2\rangle$ from the value of Δ_{LW} using standard expressions, (Polnaszek and Freed, 1975; Freed et al., 1994), and we obtain estimates that are reasonably consistent with the value of $\langle\theta_0^2\rangle = 0.04$ reported by Stohrer et al. (1991) from an analysis of NMR T_2 values in DMPC. Thus it seems reasonable that the slow process we see is that of ODF. [Rommel et al. (1988) also analyze another slow process, that of translationally induced rotations by diffusion of molecules along vesicles with finite radius of curvature (see also Liang et al., 1993). However, they find this mechanism has a correlation time of 5×10^{-6} s, which is an order of magnitude longer than what we observe for the slow process (cf. Table 4), and they argue that only ~5% of the structures have defects causing this, which would also not be consistent with our observations].

The observation of ODF in "real time" in a 2D-ELDOR experiment is complementary to NMR, wherein ODF manifest themselves in the spin relaxation, i.e., T_1 and T_2. It is

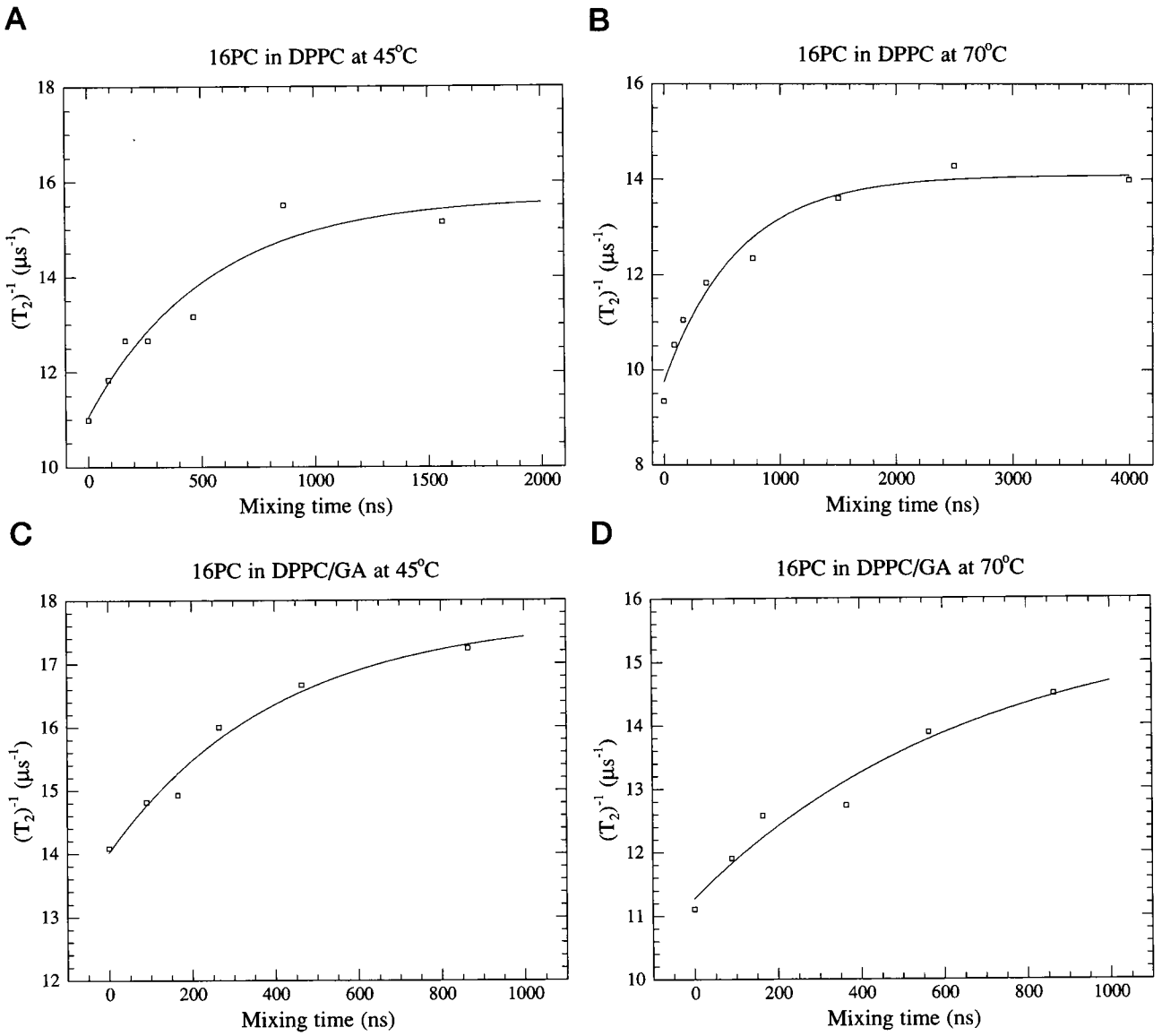

FIGURE 14 Apparent T_2^{-1} plotted as function of mixing time, and the least squares fit to Eq. 1: (*A*) 16-PC in DPPC at 45°C; (*B*) 16-PC in DPPC at 70°C; (*C*) 16-PC in DPPC/GA at 45°C; (*D*) 16-PC in DPPC/GA at 70°C.

possible in the 2D-ELDOR experiment to separately determine the extent of the fluctuations (i.e., the $\langle\theta_0^2\rangle$) and the relaxation time(s) associated with the process. Actually, the general (hydrodynamic) theory for such processes (de Gennes, 1974; Freed, 1977; Marqusee et al., 1984; Stohrer et al., 1991; Freed et al., 1994) involves a continuum of relaxation times once the ODF are analyzed in Fourier space. In particular, one finds for the qth Fourier component, the relaxation time $\tau_q = \eta/Kq^2$ and mean-square fluctuation $\langle q_q^2\rangle = k_B T/d\lambda_l^2 Kq^2$ where η is the effective viscosity, K is an average force constant, d is the bilayer thickness, and λ_l is the long wavelength cutoff of the modes. Our experimental results were successfully analyzed in terms of a single relaxation time, τ_c (cf. Eq. 1), which is reasonable considering the limited time and orientational resolution of the experiment. That is we see a growing-in of the IB according to a simple rate process, given by $1 - \exp(-T_m/\tau_c)$. This corresponds to a rerandomization of a

TABLE 4 Fitting parameters for line broadening in ELDOR experiments*

Sample	Temp. (°C)	T_2^{-1} ($10^6 s^{-1}$)	Δ_{LW}($10^6 s^{-1}$)	τ_c (ns)
DPPC	70#	9.7	4.3	640
DPPC	45§	11.1	3.8	370
DPPC/GA	70#	11.3	4.4	670
DPPC/GA	45§	14.5	4.0	400

*Experimental fit to Eq. 1.
#Data fit to average linewidth for the $m_I = 1$ and $m_I = 0$ lines.
§Data fit to $m_I = 1$ line.

local director that was oriented at some initial value ψ_0 with the correlation time τ_c (Freed, 1977). From the above expressions, we see that the mean-square fluctuation $\langle\theta_q^2\rangle$ is largest and the relaxation time, τ_q, is the slowest for the smallest value of q, which is $q_l = 2\pi/2\lambda_l$. It is reasonable to suppose, therefore, that the long wavelength modes at or near λ_l will dominate in our observations. [The high-q-modes, comparable to molecular dimension, will relax too rapidly and be of such small amplitude as to be unimportant]. We thus identify τ_c as $\sim\tau_l = \lambda_l^2\eta/4\pi^2K$. If we use the experimental estimates of $\eta = 0.1\ P$ and $K = 2 \times 10^{-11}\ N$ (Stohrer et al., 1991), then we get $\tau_l = 1.3 \times 10^7\lambda_l^2$. Thus for $\tau_c \sim 4 \times 10^{-7}\ s^{-1}$ (cf. Table 4), one has $\lambda_l \sim 1.8 \times 10^{-7}$ m. This is a value intermediate between the values estimated by Stohrer et al. (1991) of $\lambda_c \sim 10^{-8}$ m for the short-wavelength cutoff and $\lambda_c \sim 8 \times 10^{-6}$ m for macroscopically aligned multilayers of DMPC. Our rough estimate of $\lambda_l \sim 0.18\ \mu$m seems more consistent with the size of the multilamellar vesicles used in this work (with diameters $\geq 1\ \mu$m), and with the estimate of Watnick et al. (1987) that the ODF encompass approximately one-third of such liposomes. One would expect greater coherence lengths, hence larger λ_l values, for the director fluctuations in macroscopically aligned samples.

Given our identification of the slow process seen in the 2D-ELDOR experiment with ODF, it is interesting to comment on the results of Table 4 in this context. The Δ_{LW} that we identify with $\langle\theta_0^2\rangle^{1/2}$ decreases slightly with decreasing temperature, and this seems consistent with the expression (de Gennes, 1974; Stohrer et al., 1991):

$$\langle\theta_0^2\rangle = [k_BT/2\pi Kd]\ln(\lambda_l/\lambda_c)$$

However, τ_c decreases substantially with decreasing temperature. If we identify τ_c with τ_l, as we have in the above, then we would expect τ_l to increase substantially with viscosity as T decreases. If, however, the coherence length of the ODF that we associate with λ_l decreases substantially as T decreases, then it is possible to rationalize our results. A decreasing λ_l could imply the growing in of defects in the vesicles as the temperature is lowered. On the other hand, the addition of GA, if anything, is seen to raise slightly the value of τ_c. Watnick et al. (1987) did conclude that the addition of a large molecule (in particular chlorophyll a) will initially disrupt the size of the cooperative domains in a membrane, but as more of the large molecule is added the cooperative distance increases again, presumably because the motions of the large molecules become correlated. They find that the force constant, K, does decrease with addition of the large molecule, but with only a slight indication of an increase in K with large concentrations of the large molecule. Further 2D-ELDOR experiments as a function of GA concentration would appear to be in order to clarify these matters.

Thus, while it seems reasonable to identify the growth in IB of the 2D-ELDOR peaks with T_m as due to ODF, some key questions remain. In this context we would recommend 2D-ELDOR studies with macroscopically aligned membranes to observe the dependence of this phenomenon on the orientation of the director with respect to the magnetic field (Freed, 1977; Stohrer et al., 1991) to better understand it.

CONCLUSIONS

1. It was shown that 2D-FT-ESR spectra provide significantly enhanced spectral resolution as compared with conventional cw-ESR spectra to the effects on the bulk lipids of adding GA to membrane vesicles.
2. There is very good agreement between the 2D-ELDOR spectra obtained as a function of mixing time, T_m, and spectral simulations based on solutions of the SLE that are fit by nonlinear least squares (NLLS) methods, especially in the liquid crystalline (L_α) phase. It is found that addition of GA to the DPPC membrane principally slows the reorientational and translational rates of the bulk lipid and only slightly increases its ordering for the 5:1 lipid to GA ratio studied.
3. In the gel phase the optimum NLLS fits are not as satisfactory. This is attributed to the simplicity of the theoretical model utilized, and to the greater spectral sensitivity to the details of the model in the slower-motional gel phase. Despite this limitation, it was found that the reorientational rate is only modestly reduced when GA is added and ordering is somewhat increased in this phase.
4. The apparent broadening of the homogeneous linewidths in real time (i.e., as a function of T_m) is analyzed in terms of cooperative order director fluctuations of the lipid molecules in the vesicle. Such a real time observation of ODF is distinct from the NMR case, wherein the effects of ODF on T_1 and T_2 must be studied. The estimates of the magnitude of this effect, and the observed relaxation rate, appear consistent with analyses based on previous NMR studies. An increase in relaxation rate with decrease in temperature, T, could be due to a reduced coherence length for ODF in the vesicles as T is reduced. Addition of GA appears to have only a small effect on the ODF for the 5:1 lipid to GA ratio studied.
5. There is no significant indication of more than one lipid species in the 2D-ELDOR spectra from GA containing vesicles despite the fact that their cw-ESR spectra have characteristic features attributable to an immobilized or boundary lipid component. An analysis of this shows that a second component would significantly affect the 2D-ELDOR if the "immobilized" component were characterized by increased ordering as proposed by Ge and Freed (1993), but would not be observable if it were characterized instead by a substantially decreased reorientational rate, provided this rate is not very slow (i.e., approaching a rate slow enough to yield rigid limit ESR spectra). This feature is indicative of the potential of 2D-FT-ESR to provide enhanced discrimination of spectral components from lipids with differing T_2 values, especially if spectrometer dead times are further reduced.

This work was supported by National Institutes of Health Grants GM25862 and RR07126, and National Science Foundation Grant CHE9313167. Theoretical spectral fitting was performed at the Cornell Theory Center and the Cornell Materials Science Center.

REFERENCES

Brown, M. F. 1982. Theory of spin-lattice relaxation in lipid bilayers and biological membranes. ^{2}H and ^{14}N quadrupolar relaxation. *J. Chem. Phys.* 77:1576–1599.

Budil, D. E., S. Lee, S. Saxena, and J. H. Freed. 1996. Nonlinear-least-squares analysis of slow-motion EPR spectra in one and two dimensions using a modified Levenberg-Marquardt algorithm. *J. Magn. Reson.* A120:155–189.

Casal, H. L., and R. N. McElhaney. 1990. Quantitative determination of hydrocarbon chain conformational order in bilayers of saturated phosphatidylcholines of various chain lengths by Fourier transform infrared spectroscopy. *Biochemistry.* 29:5423–5427.

Cassol, R., A. Ferrarini, and P. L. Nordio. 1993. Dynamics of nitroxide probes linked to flexible chains. *J. Phys. Chem.* 97:2933–2940.

Cassol, R., M. Ge, A. Ferrarini, and J. H. Freed 1997. Chain dynamics and the simulation of ESR spectra from oriented phospholipid membranes. *J. Phys. Chem.* 101: (in press).

Cornell, B. A., L. E. Wier, and F. Separovic, 1988. The effects of gramicidin A on phospholipid bilayers. *Eur. Biophys. J.* 16:113–119.

Crepeau, R. H., S. Saxena, S. Lee, B. Patyal, and J. H. Freed. 1994. Studies of lipid membranes by two-dimensional Fourier transform ESR: enhancement of resolution to ordering and dynamics. *Biophys. J.* 66: 1489–1504.

de Gennes, P. G. 1974. The Physics of Liquid Crystals. Oxford University Press, New York.

Devaux, P. F., and M. Seignenret. 1985. Specificity of lipid-protein interactions as determined by spectroscopic techniques. *Biochim. Biophys. Acta.* 822:63–125.

Earle, K. A., J. K. Moscicki, M. Ge, D. E. Budil, and J. H. Freed. 1994. 250 GHz-ESR studies of polarity gradients along the aliphatic chains in phospholipid membranes. *Biophys. J.* 66:1213–1221.

Ferrarini, A., P.-L. Nordio, G. T. Moro, R. H. Crepeau, and J. H. Freed. 1989. A theoretical model of phospholipid dynamics in membranes. *J. Chem. Phys.* 91:5707–5721.

Freed, J. H. 1977. Stochastic-molecular theory of spin-relaxation for liquid crystals. *J. Chem. Phys.* 66:4183–4199.

Freed, J. H. 1987. Molecular rotational dynamics in isotropic and oriented fluids studied by ESR. *In* Rotational Dynamics of Small and Macromolecules in Liquids. T. Dorfmuller and R. Pecora, editors. Springer-Verlag, Berlin, Germany. 89–142.

Freed, J. H., A. Nayeem, and S. B. Rananavare. 1994. ESR studies of molecular dynamics at phase transitions in liquid crystals. *In* The Molecular Dynamics of Liquid Crystals. G. R. Luckhurst and C. A. Veracini, editors. Kluwer, Dordrecht, The Netherlands. 335–364.

Gamliel, D., and J. H. Freed. 1990. Theory of two-dimensional ESR with nuclear modulation. *J. Magn. Reson.* 89:60–93.

Ge, M., D. B. Budil, and J. H. Freed. 1994. ESR studies of spin-labeled membranes aligned by isopotential spin-dry ultracentrifugation: lipid-protein interactions. *Biophys. J.* 67:2326–2344.

Ge, M., and J. H. Freed. 1993. An ESR study of interactions between gramicidin A′ and phosphatidylcholine bilayers. *Biophys. J.* 65: 2106–2123.

Gorcester, J., and J. H. Freed. 1988. Two-dimensional Fourier transform ESR correlation spectroscopy. *J. Chem. Phys.* 88:4678–4693.

Gorcester, J., G. L. Millhauser, and J. H. Freed. 1989. Two-dimensional and Fourier transform ESR: *In* Advanced EPR Applications in Biology and Biochemistry. A. J. Hoff, editor. Elsevier, Amsterdam. 177–242.

Gorcester, J., G. L. Millhauser, and J. H. Freed. 1990. Two-dimensional electron-spin resonance. *In* Advances in Pulsed and Continuous Wave Electron Spin Resonance. L. Kevan and M. Bowman, editors. Wiley, New York. 119–194.

Hwang, J. S., R. P. Mason, L. P. Hwang, and J. H. Freed. 1975. ESR studies of anisotropic rotational reorientation and slow tumbling in liquid and frozen media III: PD-tempone and an analysis of fluctuating torques. *J. Phys. Chem.* 79:489–511.

Jost, P. C., O. H. Griffin, R. A. Capaldi, and G. A. Vanderkooi. 1973. Evidence for boundary lipid in membranes. *Proc. Natl. Acad. Sci. USA.* 70:480–484.

Kar, L., E. Ney-Igner, and J. H. Freed. 1985. Electron spin resonance and electron-spin echo study of oriented multilayers L_{α}-phosphatidylcholine water systems. *Biophys. J.* 48:569–595.

Knowles, P. F. A., W. Watts, and D. Marsh. 1979. Spin-labeled studies of lipid immobilization in dimyristoylphosphatidylcholine-substituted cytochrome oxidase. *Biochemistry.* 18:4480–4487.

Liang, Z., P. O. Westlund, and G. J. Wikander. 1993. A quantitative ESR lineshape study of the local motion in the micellar and liquid crystalline lamellar phases of the oleoyllysolecithin water system. *J. Chem. Phys.* 99:7098–7107.

Lee, S., D. E. Budil, and J. H. Freed. 1994b. Theory of two-dimensional Fourier transform ESR for ordered and viscous fluids. *J. Chem. Phys.* 101:5529–5558.

Lee, D. C., A. A. Durrani, and D. Chapman. 1984. A difference infrared spectroscopic study of gramicidin a, alamethicin, and bacteriorhodopsin in perdeuterated dimyristoyl phosphatidyl choline. *Biochim. Biophys. Acta.* 769:49–56.

Lee, S., B. R. Patyal, and J. H. Freed. 1993. A two-dimensional Fourier transform electron-spin resonance (ESR) study of nuclear modulation and spin relaxation in irradiated malonic acid. *J. Chem. Phys.* 98: 3665–3689.

Lee, S., B. R. Patyal, S. Saxena, R. Crepeau, and Jack H. Freed. 1994a. Two-dimensional Fourier transform electron-spin resonance in complex fluids. *Chem. Phys. Lett.* 221:397–406.

Marqusee, J. A., M. Warner, and K. A. Dill. 1984. Frequency dependence of NMR spin lattice relaxation in bilayer membranes, *J. Chem. Phys.* 81:6404–6405.

Marsh, D. 1985. ESR probes for structure and dynamics of membranes. *In* Spectroscopy and Dynamics of Molecular and Biological Systems. P. M. Bayley and R. E. Dale, editors. Academic, London, UK. 209–238.

Marsh, D. 1989. Experimental methods in spin-label spectral analysis. *In* Biological Magnetic Resonance. Vol. 8. L. J. Berliner and J. Reuben, editors. Plenum Press, New York. 255–303.

Marsh, D., and A. Watts. 1982. Spin labeling and lipid-protein interactions in membranes. *In* Lipid-Protein Interactions. P. C. Jost and O. H. Griffith, editors. John Wiley and Sons, New York. 53–126.

Meirovitch, E., A. Nayeem, and J. H. Freed. 1984. An analysis of protein-lipid interactions based on model simulations of ESR spectra. *J. Phys. Chem.* 88:3454–3465.

Millhauser, G. L., J. Gorcester, and J. H. Freed. 1987. New time-domain EPR methods for the study of slow motions on surfaces. *In* Electronic Magnetic Resonance of the Solid State. J. A. Weil, editor. Canadian Society of Chemistry, Ottawa, Canada. 571–597.

Patyal, B. R., R. H. Crepeau, D. Gamliel, and J. H. Freed. 1990. Two-dimensional Fourier transform ESR in the slow motional and rigid limits: SECSY-ESR. *Chem. Phys. Lett.* 175:445–452.

Polnaszek, C. F., and J. H. Freed. 1975. ESR studies of anisotropic ordering, spin relaxation, and slow tumbling in liquid crystalline solvents. *J. Phys. Chem.* 79:2283–2306.

Rice, D., and E. Oldfield. 1979. Deuterium nuclear magnetic resonance studies of the interaction between dimyristoyl phosphatidylcholine and gramicidin A. *Biochemistry.* 18:3272–3279.

Rommel, E., F. Noack, P. Meier, and G. Kothe. 1988. Proton spin relaxation dispersion studies of phospholipid membranes. *J. Phys. Chem.* 92:2981–2987.

Sastry, V. S. S., A. Polimeno, R. H. Crepeau, and J. H. Freed. 1996a. Studies of spin relaxation and molecular dynamics in liquid crystals by 2D-FT-ESR. I. Cholestane in butoxyl-benzylidene-octylaniline and dynamic cage effects. *J. Chem. Phys.* 105:5753–5772.

Sastry, V. S. S., A. Polimeno, R. H. Crepeau, and J. H. Freed. 1996b. Studies of spin relaxation and molecular dynamics in liquid crystals by 2D-FT-ESR II. Perdeuterated tempone in butoxyl-benzylidene-octylaniline and dynamic cage effects. *J. Chem. Phys.* 105:5773–5791.

Schneider, D. J., and J. H. Freed. 1989. Calculating slow motional magnetic resonance spectra: a user's guide. *In* Biological Magnetic Resonance. Vol. 8. L. J. Berliner and J. Reuben, editors. Plenum Publishing Corp., New York. 1–76.

Shin, Y.-K., and J. H. Freed. 1989. Dynamic imaging of lateral diffusion by electron spin resonance and study of rotational dynamics in model membranes. *Biophys. J.* 55:537–550.

Short, K. W., B. A. Wallace, R. A. Myers, S. P. A. Fodor, and A. K. Dunker. 1987. Comparison of lipid/gramicidin dispersions and cocrystals by Raman scattering. *Biochemistry.* 26:557–562.

Stohrer, J., G. Gröbner, D. Reimer, K. Weisz, C. Mayer, and G. Kothe. 1991. Collective lipid motions in bilayer membranes studied by transverse deuteron spin relaxation. *J. Chem. Phys.* 95:672–678.

Tanaka, H., and J. H. Freed. 1985. Electron spin resonance studies of lipid-gramicidin interactions utilizing oriented multilayers. *J. Phys. Chem.* 89:350–360.

Watnick, P. I., P. Dea, and S. I. Chan. 1990. Characterization of the transverse relaxation rates in lipid bilayers. *Proc. Natl. Acad. Sci. USA.* 87:2082–2086.

Watnick, P. I., P. Dea, A. Nayeem, and S. I. Chan. 1987. Cooperative lengths and elastic constants in lipid bilayers: the chlorophyll a/dimyristoyl lecithin system. *J. Chem. Phys.* 86:5789–5800.

Watts, A., I. D. Volotovski, and D. Marsh. 1979. Rhodopsin-lipid associations in bovine rod outer segment membranes. Identification of immobilized lipid by spin-labels. *Biochemistry.* 18:5006–5013.

Williams, B. W., and C. D. Stubbs. 1988. Properties influencing fluorophore lifetime distributions in lipid bilayers. *Biochemistry.* 27: 7994–7999.

Xu, D., R. H. Crepeau, C. K. Ober, and J. H. Freed. 1996. Molecular dynamics of a liquid crystalline polymer studied by 2D-FT and cw ESR. *J. Phys. Chem.* 100:15873–15885.